ＩＳＳＮ１３４６－７８３２

独立行政法人港湾空港技術研究所

港湾空港技術研究所報告

REPORT OF THE PORT AND AIRPORT RESEARCH INSTITUTE

VOL.49　NO.2　June 2010

NAGASE, YOKOSUKA, JAPAN

INDEPENDENT ADMINISTRATIVE INSTITUTION,
PORT AND AIRPORT RESEARCH INSTITUTE

港湾空港技術研究所報告（REPORT OF PARI）

第 49 巻　第 2 号（Vol. 49，No. 2），　2010年6月（June 2010）

目　　次（CONTENTS）

REPORT OF THE PORT AND
AIRPORT RESEARCH INSTITUTE
Vol.49 , No.2 (Jun.2010)

Hysteresis loop model for the estimation of the coastal water temperatures - by using the buoy monitoring data in Mikawa Bay, JAPAN -

Hong Yeon CHO *
Kojiro SUZUKI **
Yoshiyuki NAKAMURA ***

Synopsis

Water temperature (hereafter WT) is one of the most important a-biotic factors influencing the distribution of marine species. It controls the rate of metabolic and reproductive activities, and determines which species can survive. However, the WT data is very poor in comparison with the air temperature (hereafter AT) data. This situation has been solved by the WT estimation method based on the regression model by using the AT data. This method, however, cannot consider the hysteresis which is the general pattern to be shown between AT and WT data relationship. It has not the time-history concept.

In this study, the Hysteresis Loop model based on the harmonic analysis is developed. It is able to consider the hysteresis pattern and includes the time-history concept. The model calibration and validation is carried out to check the RMS error by using the 4-year period (2005. 7- 2009. 6) AT and WT data of the monitoring buoy in Mikawa bay. The results show that the RMS error of the WT estimation only using the AT data is in the range of 0.8 – 1.0 at the calibration and validation stage. It is better in comparison with the RMS error 1.4-2.1 of the linear regression model.

The Hysteresis Loop model can be used as an efficient tool for the prediction of the present and near future WT in the coastal area. It can be regarded to predict the more accurate and reliable WT information in the condition of the WT rise in the (near) future due to the global warming effects

Key Words: Hysteresis Loop model, air temperature, water temperature, harmonic analysis, hysteresis, Mikawa Bay.

* Visiting Scientist of Ocean Environment Information Research Team

** Team Leader of Ocean Environment Information Research Team

*** Director of Special Research

Port and Airport Research Institute, 3-1-1 Nagase, Yokosuka, Kanagawa, 239-0826, Japan

Phone：+81-46-844-5049 Fax：+81-46-844-1274 e-mail: cho-h@pari.go.jp and/or hycho@kordi.re.kr

港湾空港技術研究所報告
第 49 巻第 2 号(2010.6)

沿岸水温を推定するヒステリシスループモデルの開発
－　三河湾ブイモニタリングデータを活用して　－

趙烘輦（チョホンヨン)*・鈴木高二朗**・中村由行***

要　旨

水温は海洋生物の代謝及び生産活動を制御してその生存可否を決めるため，海洋生物に影響を及ぼす最も重要な環境因子である．しかし，水温は気温に比べてデータが著しく少ないため，これまでは回帰分析を用いて気温から水温を推定するということが行われてきた.ただし，既存の回帰分析では，気温と水温の履歴現象を考慮できないため，推定値が大きく異なる場合が多い.

そこで，本研究では調和解析を含んだヒステリシスループモデル（履歴循環モデル）を開発した．このモデルは履歴現象を考慮することができるとともに，時系列の概念を含んでいる．ここでは，本モデルを三河湾にあるモニタリングブイの 4 年間(2005．7 - 2009．6)の 気温および水温データに適用してモデルの精度を調べた．その結果，推定値と観測値の RMS 誤差は 0.8 - 1.0 と小さく，推定値と観測値でよい一致をみた．また，この結果は既存の線形回帰モデルの RMS 誤差である 1.4－2.1 に比べて小さかった.

本研究で開発された履歴循環モデルは，現在及び近未来の沿岸の水温を予測するうえで，効果的なツールとして活用されるものと期待される.

キーワード：履歴循環モデル（HL モデル)，気温，水温，沿岸，調和解析，三河湾

*　客員研究員（KORDI）

**　海洋環境情報研究チームリーダー

*** 研究主監

〒239-0826　神奈川県 横須賀市 長瀬　3-1-1,　独立行政法人港湾空港技術研究所

電話：046-844-5049　Fax：046-844-1274　e-mail: cho-h@pari.go.jp and/or hycho@kordi.re.kr

Contents

1. Introduction

Water temperature is one of the most important physical properties of the coastal and marine environment as it has a direct/indirect influence on many physical, chemical, and biological processes (Lalli & Parsons, 1997). It also exerts major influence on aquatic organisms with respect to selection/occurrence and level of activity of the organisms. Water temperature is important because it governs the kinds of aquatic life that can live in a stream and the coastal seas (Murphy, 2009). Fish, zooplankton, phytoplankton, and other aquatic species all have a preferred temperature range. If temperature gets too far above or below this preferred range, the number of individuals of the species decreases until finally there are none (Department of Ecology, State of Washington, 2009).

Temperature controls the rates at which chemical reactions and biological processes (such as metabolism and growth) take place. Temperature and salinity variations combine to determine the density of seawater, which in turn greatly influences vertical water movements with consequent changes in chemical and biological processes within the water column and the surface sediment layer (Lalli & Parsons, 1997). Water temperature partly determines the concentration of dissolved gases in seawater; these include oxygen and carbon dioxide, which are profoundly linked with biological processes. Temperature is also one of the most important a-biotic factors influencing the distribution of marine species (Lalli & Parsons, 1997). It controls the rate of metabolic and reproductive activities, and determines which fish species can survive (Murphy, 2009). It also affects the concentration of dissolved oxygen and can influence the activity of bacteria and toxic chemicals in water (Murphy, 2009). It is an essential factor of the study on the heat budget computation in the semi-enclosed bays, the shallow coastal zone, and the marginal seas (Hsu, 1988).

As expected, an increase in the importance of the public natural resources, such as the open ocean space, the beach, the natural habitats in the coastal zone, etc., leads to a great attention to their intangible values in the coastal seas. Water temperature is an essential factor for the aquatic environment and the fishery resources management (Crisp and Howson, 1982; Poff et al., 2002; Weber et al., 2007).

Furthermore, the change of the coastal water temperature is most probably expected in the (near) future because of the global warming effects. Its change also has an effect on the coastal ecosystem and would act as a limiting factor for the coastal utilization of human beings because it is very important and critical factor on the aquatic environment in the shallow coastal zone (UNEP, 2007).

However, there is a practical limitation in the estimation of the long-term water temperature change by using the available long-term water temperature data because they are not available in most cases. Thus, it is highly recommended that the water temperature changes should be estimated by using the air temperature data, for water temperature data are relatively poor and not sufficient to estimate its future changes in comparison with the air temperature data. In relation to this, the study on the water temperature estimation has been carried out mainly focused on the stream temperatures (Stefan and Preud'home, 1993; Pilgrim and Stefan, 1995; Morrill et al., 2005; Cho et al., 2007; Benyahya et al., 2007).

On the contrary, the study on the estimation of the coastal water temperatures is very limited because there are no sufficient continuous monitoring data in the bay or coastal areas. The numerical models based on the energy conservation concept (the heat balance in the simulation area) are widely used to simulate the distribution of the spatial and temporal water temperatures in the lakes, streams, and coastal areas. It requires many input data set, e.g., solar radiation or sun light time, rainfall and snow fall, wind velocity and direction, humidity, air pressure, topography, altitude and longitude, and air and water temperatures of the simulation area, etc. Although these mechanism-based models might be more accurate than statistical models, the accuracy of its simulation results highly depends on the input data conditions and the condition of the complete input data set for model run is rarely satisfied and thus unavailable input data should be estimated based on the regression model.

The relationship-type model only using the air and water temperatures data is highly recommended and

practically accepted if the reliability of the water temperature's estimation is in the acceptable level based on the project target. First of all, the variations between air and surface water temperatures have very similar patterns in an overall point of view (Knauss, 1979; Berner and Berner, 1987). It makes the construction of the air and water temperature's relationship possible.

In general, the studies on the water temperature estimation have been conducted based on the simple linear regression model or the non-linear S-shape curve (logistic) model (Benyahya et al., 2007; Morrill et al., 2005; Mohseni et al., 1998; Cho et al., 2007; Lee, 2007). It is a kind of stochastic model. In general, the data-division method is used in order to consider the hysteresis (time-lag response) which is the general pattern to be shown between air and water temperature data relationship. This method is composed of the 2 steps, the data-division step dividing the total data period into a temperature rising and falling intervals based on the specified criteria, and the model parameters estimation step using the divided data, respectively (Kyle & Brabets, 2001). However, the research on the coastal water temperature estimation model is very limited because of the available data condition. The estimation model for the surface water temperature in the coastal zone are suggested as the linear and non-linear regression model and the hysteresis pattern between air and water temperatures are analyzed in detail (Cho et al., 2007; Lee, 2007). However, only surface water temperatures data are used because there is no bottom water temperature data and the estimation method is basically based on the regression analysis in their study. There is no time-series concept.

In this study, the hysteresis loop (hereafter HL) model, which integrates the air temperature rising and falling intervals and is constructed based on the traditional harmonic analysis method, is suggested as the more reliable coastal water temperature estimation model. The error bounds of the estimation using this HL model is computed and compared to the error bounds of the simple linear regression model. In order to improve the HL model application level, the relationship of the dominant harmonic constants between the air and water temperatures with respect to the difference and ratio is analyzed in detail and suggests the model application methods in relation to the future air temperature changes.

2. Variation pattern analysis between air and water temperatures – Mikawa bay buoy Data

The air and water temperature's time-series data have a dominant annual and a less dominant inter-annual variation patterns even though they have different shapes which is considered as the time-lag response effects due to the air-water specific heat or hear capacity and the heat transfer efficiency in the water column. It can be easily shown from the time-series plot and scatter plot of the air and water temperature data set. In this analysis, we used the buoy monitoring data in Mikawa bay located in the eastern part of the Ise Bay.

There are air and coastal water temperatures data set in Mikawa bay, Japan. It has been continuously measured in the 3 automatic monitoring buoys installed in the Mikawa Bay and operated by the Fishery Experiment Station, Aichi Prefecture from July 1st, 2003 until now. Fig. 1 shows the location of the monitoring buoy and Japan Meteorological Agency (hereafter JMA) Irago weather monitoring stations.

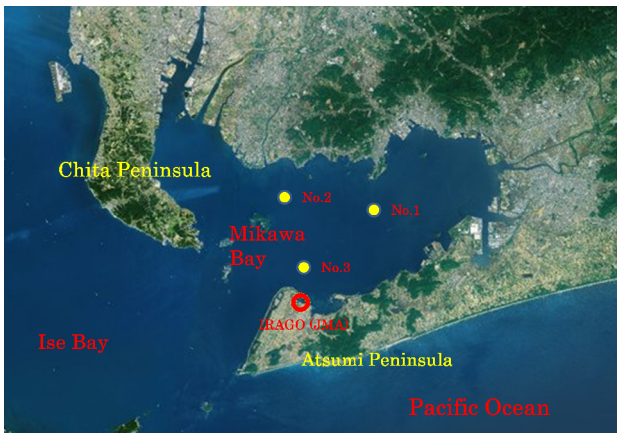

Fig. 1 Location of the Coastal Monitoring Buoy and Irago Weather Monitoring Station (JMA) in Mikawa Bay (Ise Bay)

Buoy 1: N 34° 44′ 36″, E137° 13′ 13″ Depth: 10.1 m.

Buoy 2: N 34° 44′ 42″, E 137° 4′ 19″, Depth: 10.0m.

Buoy 3: N 34° 40′ 30″, E 137° 5′ 49″, Depth: 13.7m.

Irago JMA Station: N 34°37′42″, E 137° 5′ 36″, Elevation: +6.2m.

Air and water temperatures including the salinity and the saturation percentage of dissolved oxygen (DO) concentration are monitored in the surface and bottom layers (Sensor positions are below 3.5m from the water surface and above 2.0m from the sea bottom, respectively) in 1-hour interval and 1-day mean (daily) data set and other supplementary data are disseminated as a *.pdf files in 10-days interval through the internet homepage (http://www.pref.aichi.jp/suisanshiken/).

There are many missing data during the beginning of the operation time because of the buoy maintenance and sensor malfunctions which have been considered as the general and common things in the coastal monitoring procedure. Taking this situation into consideration, the air and water temperatures data during the recent 4 years (2005.7.–2009.6) having a relatively small missing data, are used in order to analyze the variation patterns. Air and water temperatures missing data are imputed (filled in) by the (stochastic) linear regression method and the Bayesian estimation method, respectively. JMA air temperature data at Irago station (in Aichi prefecture) which can be downloaded through the Internet website (www.jma.go.jp) are used to impute the missing air temperatures of the monitoring buoys. Although there are many missing data imputation methods (techniques), whether which methods are selected and used (applied) or not, the impacts on the information of the data is expected not so serious because the data missing ratio is about below 5% or much less (Little & Rubin, 2002). To use all available data (6-year's data) is better to analyze the long-term variation pattern. However, only 4 year's data having a relatively small missing data are used because the many missing data could lead to the bias like an outlier and loss of precision in case of using these kind of data(Little & Rubin, 2002; Barnett & Lewis, 1994).

As a 1st step, the basic statistical information of the each buoy data and Irago JMA station data are computed and their time-series data plot and correlation functions are displayed. (See the Table 1 and Figure 2-4). Table 1 shows the data missing ratio is about below 5%, the highest mean value of the temperatures is the surface water temperature, and whereas the highest standard deviation value of the temperatures is the air temperatures. The general pattern that the water temperatures are higher than air temperatures on the average value is only applied to the surface water temperature. It is not true to the bottom water temperatures because the annual-mean bottom water temperatures are nearly close to the annual-mean air temperatures in this case.

Fig. 2 shows the time-series plot of the air temperatures data of the 3 buoys and JMA station. It shows the difference between air temperature data is very small and the determination coefficient (R^2) between JMA and buoy air temperatures are computed above 0.99 based on the regression analysis. The standard deviation between the JMA and Buoy 1, 2, and 3 air temperatures data are 0.6785, 0.5935, and 0.6431, respectively. It means that the JMA air temperature is very close to the Buoy's air temperatures data. The basic regression results, i.e., the regression curve and R^2 value are summarized as follows:

$(AT)_{B1} = 1.0003\ (AT)_{JMA}+0.1008$, $R^2=0.9922$,

$(AT)_{B2} = 0.9946\ (AT)_{JMA}+0.0048$, $R^2=0.9938$,

$(AT)_{B3} = 0.9737\ (AT)_{JMA}+0.5662$, $R^2=0.9931$,

where, AT is the air temperature and the subscripts JMA, B1, B2, and B3 refers to the JMA, Buoy 1, Buoy 2, and Buoy 3, respectively.

These equations of each regression curve can be used to estimate the buoy air temperatures relatively having many missing data because the JMA data, nearly no-missing data, are highly correlated with the air temperature data of the buoy.

Figures 3 and 4 show the comparison time-series plots of the temperature data in each buoys and the air and water temperatures data of all buoy, respectively. In this case, all the available data (2003.7.1.-2009.10.30.) are plotted to check the missing condition, the clear annual variation and the fluctuation pattern, and the thermal stratification between surface and bottom water temperatures in Fig. 3. As shown in Figure 3, the time-lag pattern between air and water temperatures also appears but not clearly because of the data fluctuation effects.

In order to check the time-memory (or history) order, the correlation analysis methods are used in this study. Figure 5 shows the auto- and cross-correlation functions between air and water temperatures.

Table 1. Basic Statistical Information of the JMA and Buoy Monitoring data

ITEMS		Mean	Standard Deviation.	Maximum temperature	Minimum temperature	No. of the missing data
AT (JMA Irago St.)		16.45	7.68	30.6	0.5	3
Buoy 1	AT	16.40	7.71	30.3	0.9	314
	Surface WT	16.84	7.41	29.9	4.2	327
	Bottom WT	15.87	6.19	26.9	4.3	346
Buoy 2	AT	15.92	7.51	29.9	1.4	142
	Surface WT	16.97	6.79	29.8	5.1	143
	Bottom WT	16.24	5.76	26.7	5.4	143
Buoy 3	AT	16.05	7.37	29.7	1.4	174
	Surface WT	16.58	6.65	29.3	5.3	199
	Bottom WT	16.35	5.66	26.4	5.5	251
AT (JMA Irago)		16.34	7.68	30.6	0.5	3
Buoy 1	AT	16.69	7.71	30.3	1.6	13
	Surface WT	16.94	7.37	29.9	4.2	26
	Bottom WT	15.93	6.09	26.9	4.3	45
Buoy 2	AT	16.34	7.67	29.9	1.4	13
	Surface WT	17.30	6.93	29.8	5.1	13
	Bottom WT	16.39	5.79	26.7	5.4	13
Buoy 3	AT	16.45	7.54	29.7	1.4	41
	Surface WT	16.85	6.77	29.3	5.3	66
	Bottom WT	16.24	5.71	25.6	5.5	47

References: The upper part information is computed by using the all available data (total data numbers = 2,191) during 2003.7.1.–2009.6.31. Whereas, the lower part information is computed by only using the data (total data numbers = 1,461) during 2005.7.1.–2009.6.30 having a relatively small missing data (below 5%). AT = air temperature, WT = water temperature.

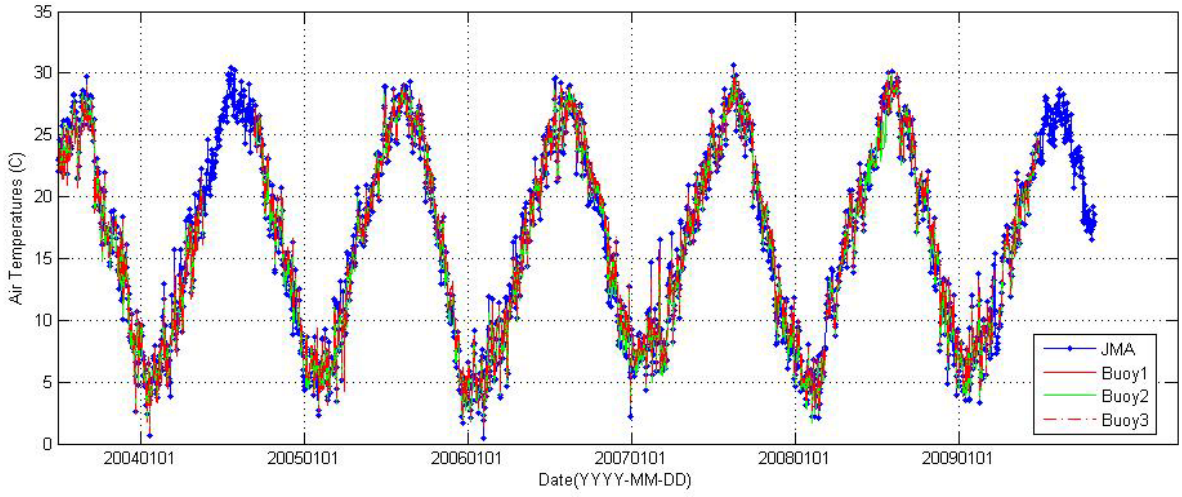

Figure 2. Time-series plot of the air temperatures in the Irago (JMA) station and the buoys.

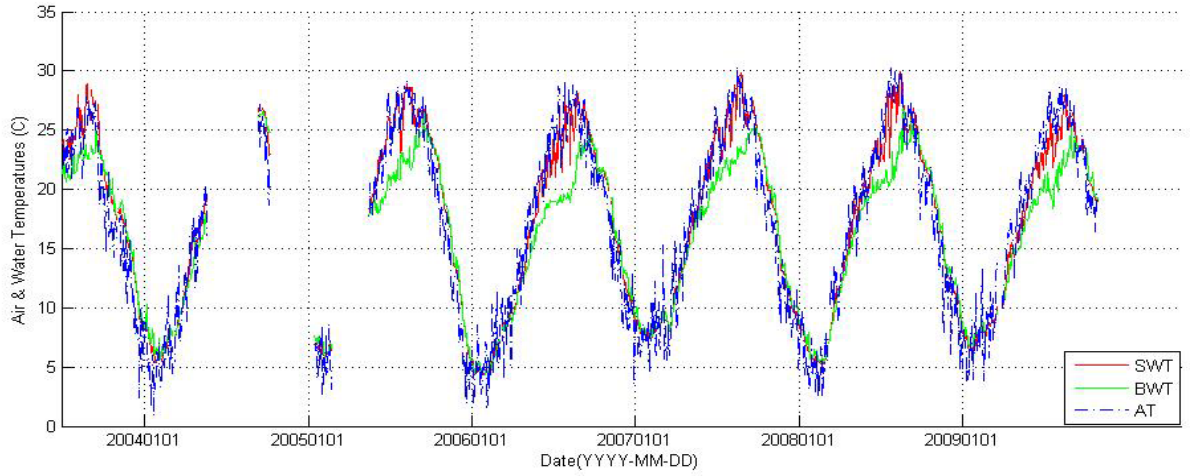

(a) Buoy 1

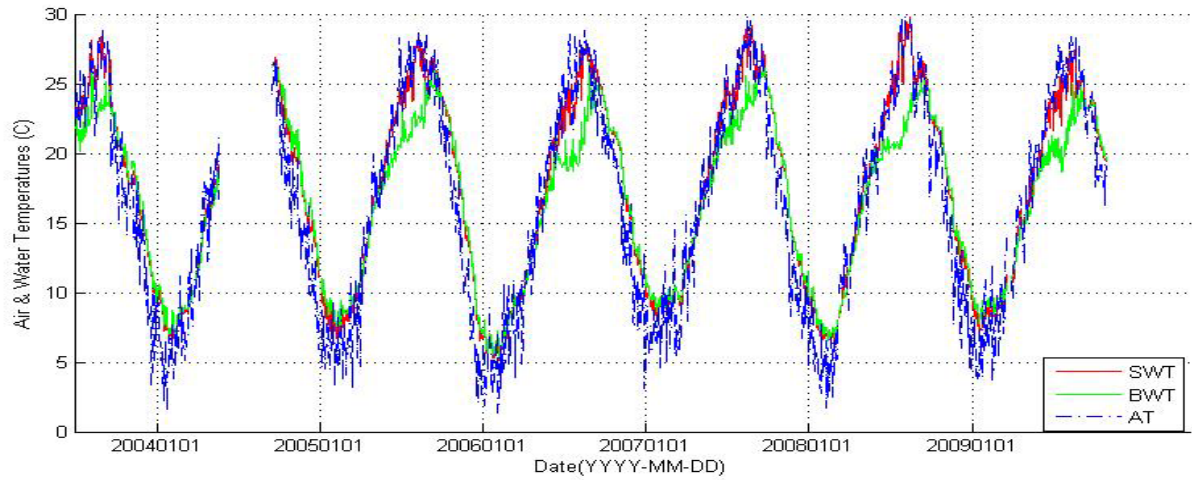

(b) Buoy 2

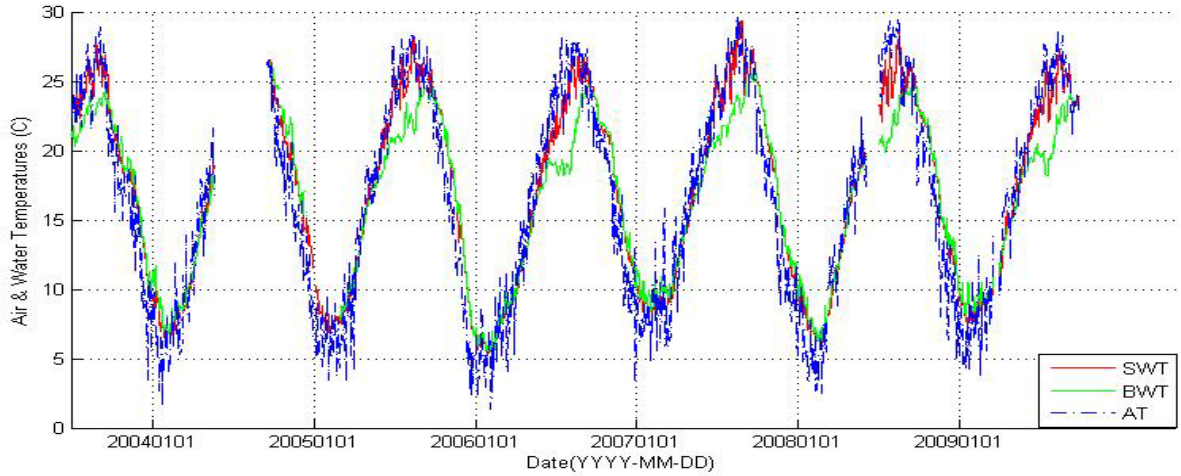

(c) Buoy 3

Figure 3. Time-series plot of the air and water temperatures data of each buoy.

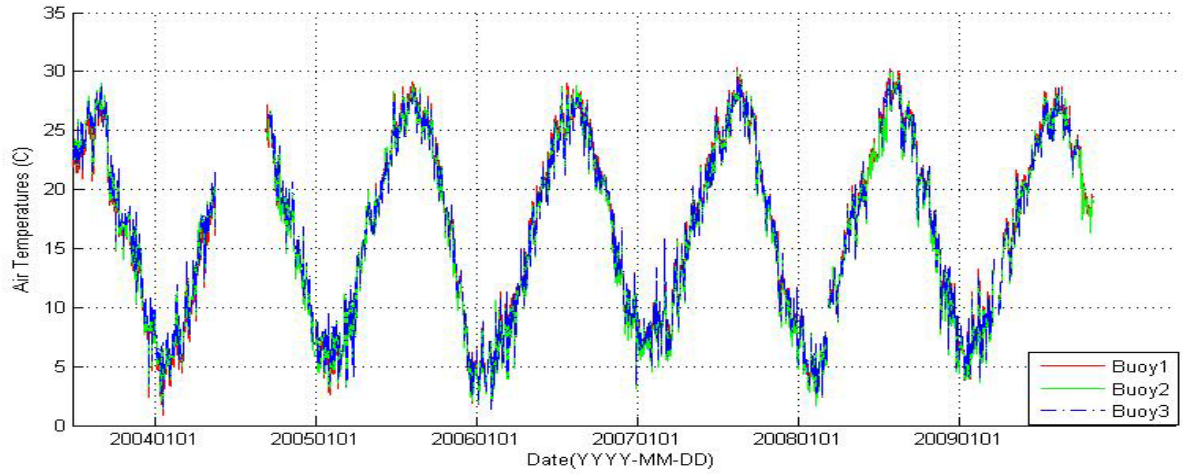

(a) Air temperatures

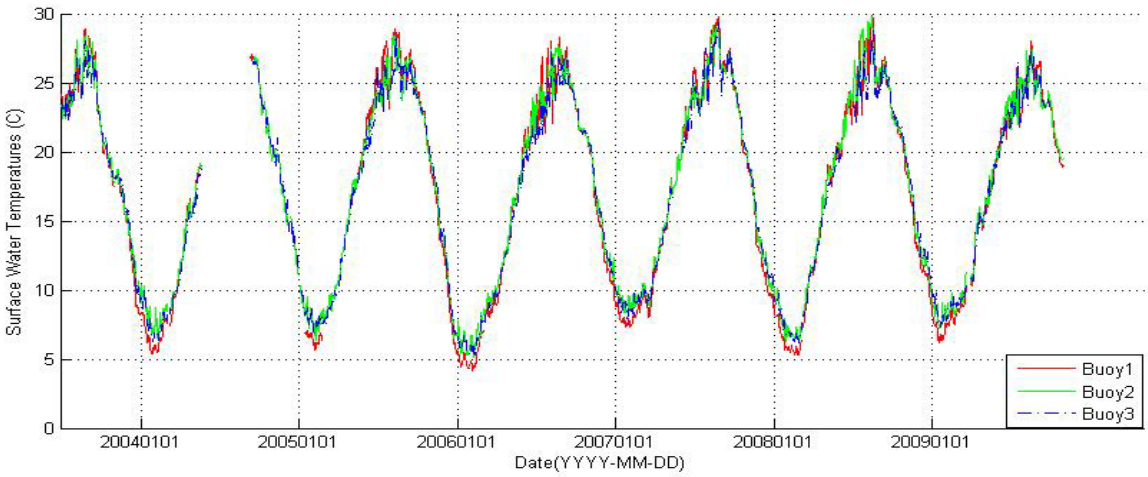

(b) Surface water temperatures.

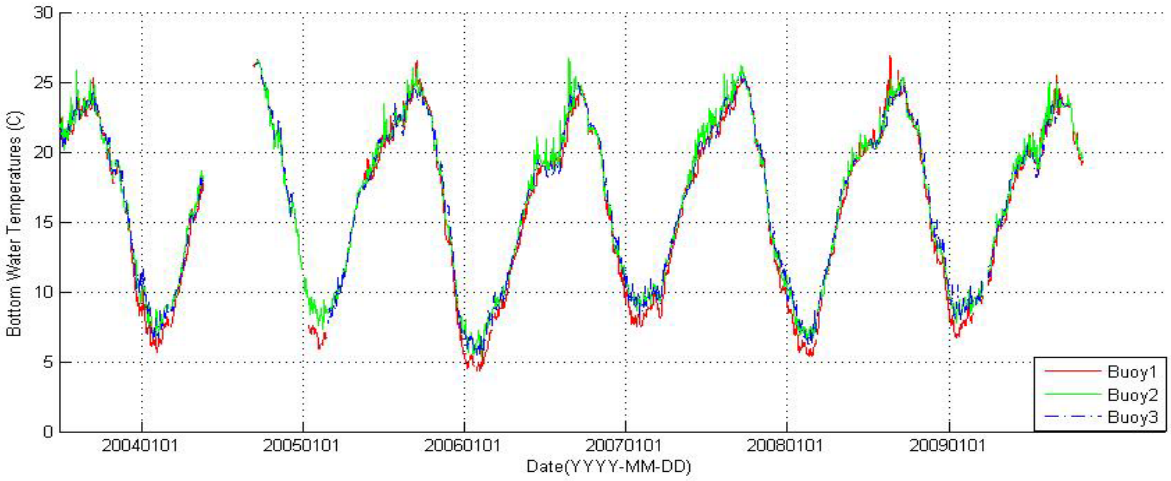

(c) Bottom water temperatures.

Figure 4. Time-series plot of the temperatures data of all buoys.

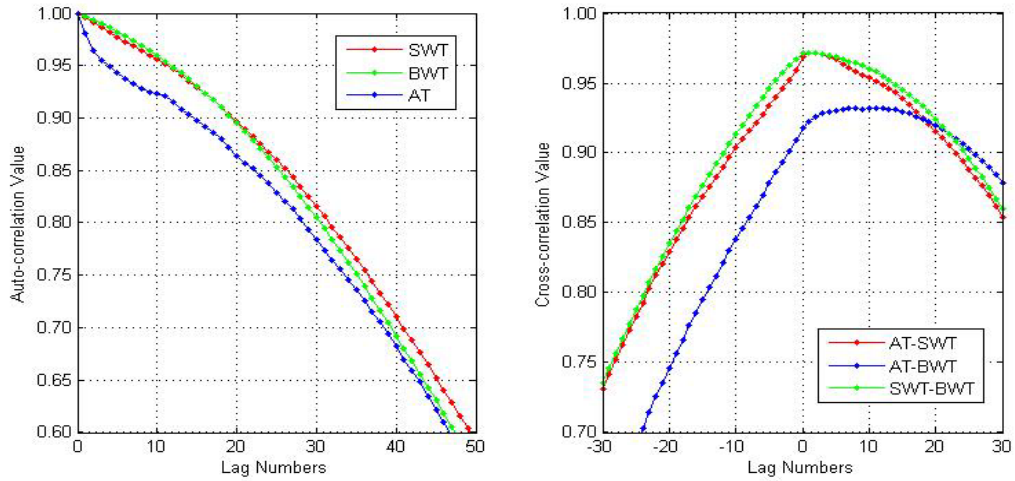

(a) Buoy 1

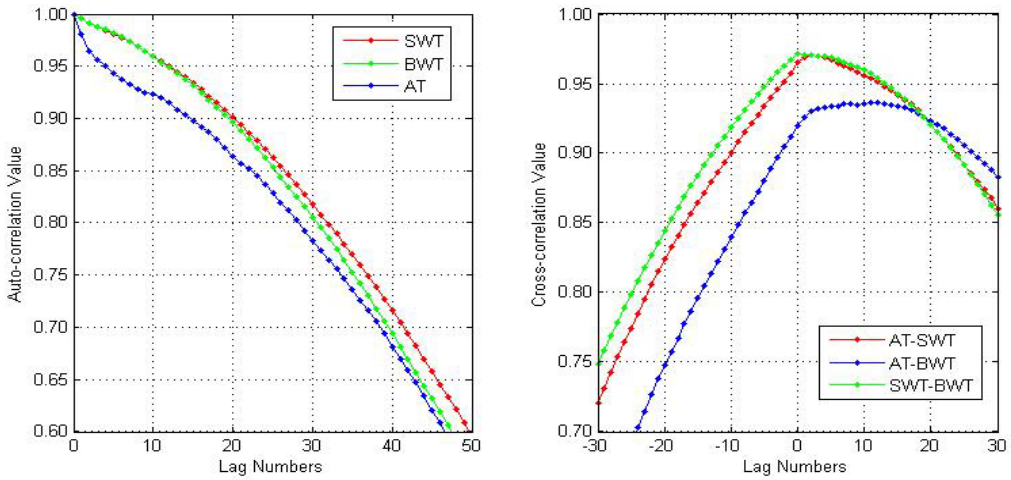

(b) Buoy 2

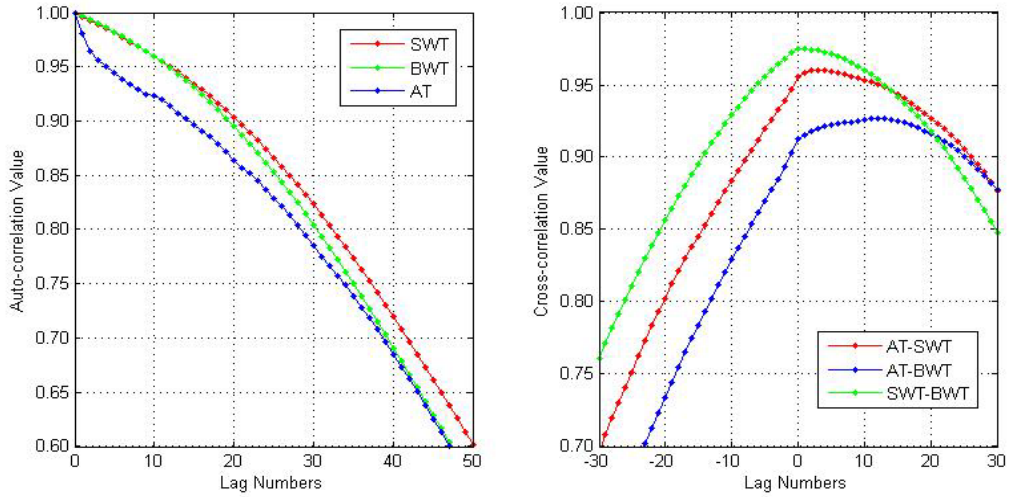

(c) Buoy 3

Figure 5. Auto- and cross-correlation functions between air and water temperatures of the buoy. (Lag Numbers Unit : days)

The values are very high even though the variation patterns have a clear difference. In general, its overall change pattern shows that the annual cycle is certainly dominant .

The auto-correlation function shows the very slow decreasing pattern and is clearly divided with 2 groups, the upper one is for the water temperature and the lower one is for the air temperature. The slow decreasing auto-correlation and cross-correlation values due to lag number mean that the data have long-memory characteristics, i.e., not negligible time-history effects neglected in the typical regression analysis.

Figure 6 shows the scatter plot between air and temperatures. As shown in this figure, the hysteresis pattern will be clearly shown between the temperatures. The hysteresis loops are constructed anti-clockwise direction in an annual cycle. The data averaged over 10 days are used in order to smooth the data fluctuation in the scatter plot. Based on the rough visual analysis of these plots, it seems that the hysteresis pattern and time-memory characteristics should be considered to analyze the relationship between air and water temperatures, and the surface and bottom water temperatures. In order to satisfy these requirements, the hysteresis loop model described in detail in the next section is developed and tested its performance with the Mikawa bay buoy monitoring data.

3. Basic concept of the hysteresis loop model

The hysteresis loop (hereafter HL) model suggested in this study is the water temperature estimation model by using the available data (air temperature in this case) having a relatively good data condition. It is mainly composed of the data smoothing and data structure comparison module. The suggested method for the data smoothing is the harmonic analysis (hereafter HA) because it considers the time-series pattern of the data. The HA used in this study is a little bit different the word used in the tidal analysis in the perspective of the frequency functions. In this study, the annual cycle and inter-annual cycle (and/or intra-annual cycle if necessary) functions are used unlikely the tidal analysis in which the M_2, S_2, K_1, O_1 and the other minor components are used. The other method for the data structure comparison is the component (or order) comparison by using the difference and/or ratio of the constants obtained by the HA. By using this method, the water temperature estimation by only using the air temperature could be possible. In relation to the hysteresis loop construction, the parametric form are suggested and used to express the loop which cannot be drawn by the single-valued curves.

4. Harmonic analysis of the temperature data

The air and water temperature data are fitted by using harmonic function based on the harmonic analysis, respectively. It is given by the summation of the harmonic functions having the different frequency terms:

$$T(t) = A_0 + \sum_{m=1}^{M}\left\{A_m \cos\left(\frac{2\pi mt}{Y}\right) + B_m \sin\left(\frac{2\pi mt}{Y}\right)\right\} + \epsilon_t \quad (1)$$

$$= A_0 + \sum_{m=1}^{M}\{A_m \cos(\omega_m t) + B_m \sin(\omega_m t)\} + \epsilon_t \quad (2)$$

in which, A_0 is the mean of the time-series data(μ_T), A_m and B_m are the harmonic coefficients of the order m, respectively, M is the maximum order of the frequency function in the harmonic analysis, ϵ_t is the residual term (error terms), and Y is the one year days (365 in a common year and 366 in a leap year; 365.25 days are used for more than 1 year). $T(t)=T_t$ are the temperature data of the t-th day, which are composed of the $T_1, T_2, \ldots, T_N$ data, in which N is the total data number of the N days. The frequency function (ω_m) used in the analysis are $2\pi(m)/Y$, in which m is the order of the harmonic analysis. The optimal order (model selection) can be determined by using the AIC (Akaike's Information Criterion) values (Kitagawa, 2005). In order to consider the long-term frequencies over 1-year, the intra-annual (n-year) periodic functions, e.g., $2\pi/(nY/2)$, could be included with ease in the harmonic analysis. Even though it makes the residual variance very low, it is skipped because it is unsuitable to analyze the long-term components by only using 4 to 6 years data.

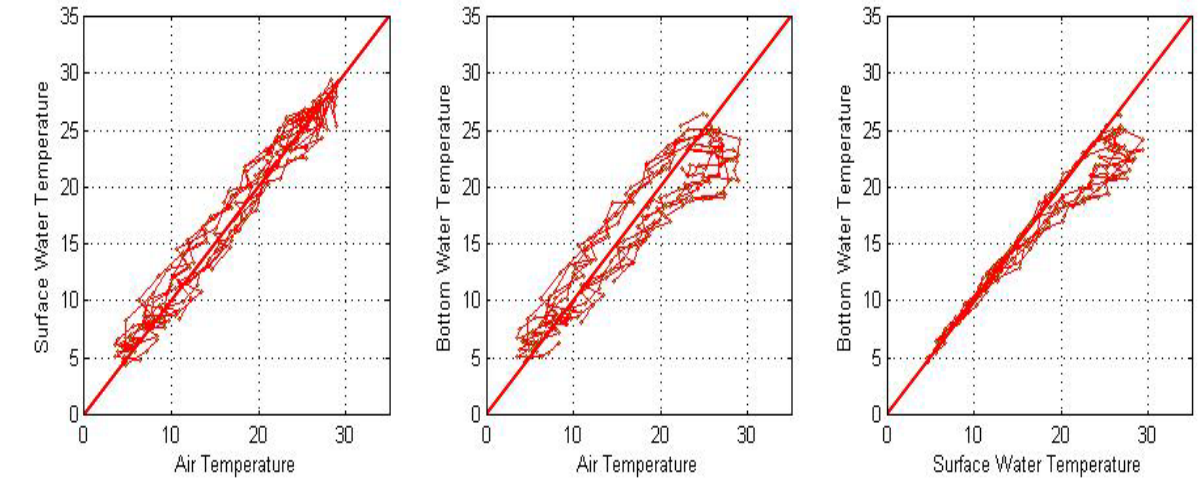

(a) Buoy 1

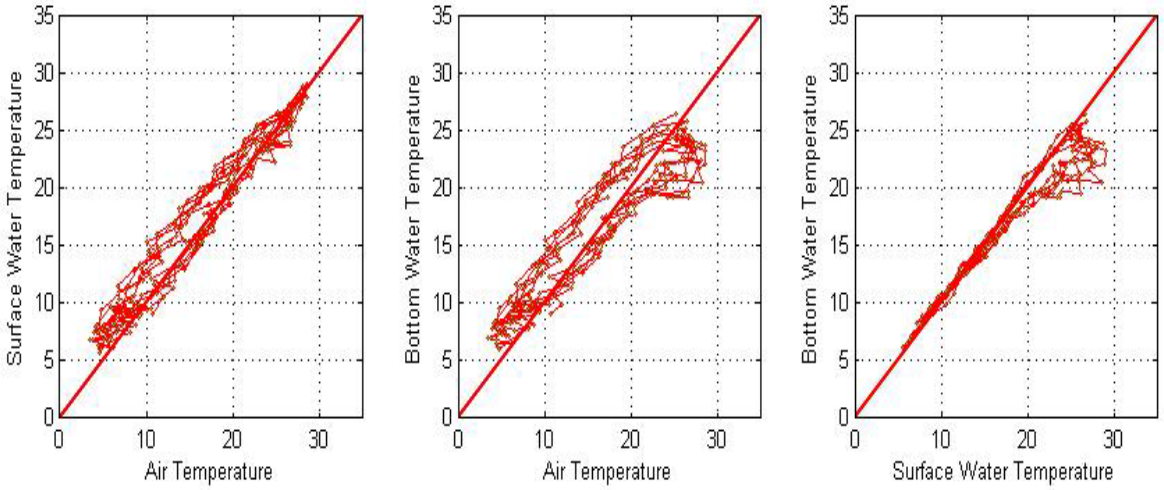

(b) Buoy 2

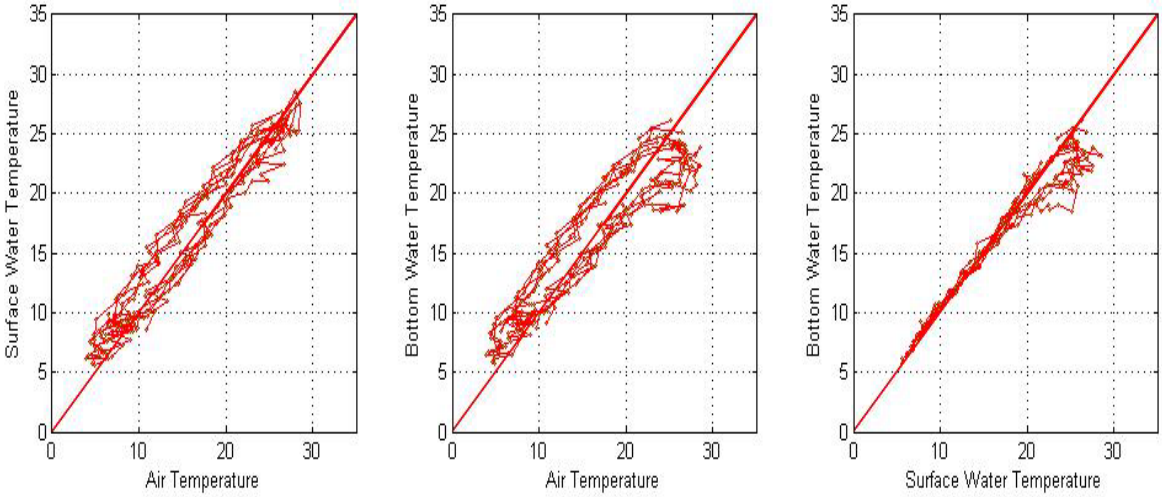

(c) Buoy 3

Figure 6. Shapes of the hysteresis loop (scatter plot) between air and water temperatures data

Table 2. The optimal order, AIC value, and variance of the residuals in the harmonic analysis.

	Buoy 1			Buoy 2			Buoy 3		
	AT	SWT	BWT	AT	SWT	BWT	AT	SWT	BWT
AIC value	4,296	3,441	3,219	4,235	3,174	3,304	4,305	3,154	3,101
M (optimal order)	35	13	12	35	11	11	32	16	10
Variance	2.59	1.20	1.06	2.45	1.02	0.90	2.64	0.98	0.95

References: AIC = Akaike Information Criterion, M = the order of the harmonic constants at the lowest AIC value, and the Variance is the variance of the difference between the observed data and the smoothed values by the harmonic analysis. AT : Air Temperature, WT : Water Temperatures, and S & B : Surface and Bottom Layers, respectively.

Table 3. Amplitude and phase information of the harmonic components in order sequences.

(a) Amplitude (°C)

Order	JMA	Buoy 1			Buoy 2			Buoy 3		
	AT	AT	SWT	BWT	AT	SWT	BWT	AT	SWT	BWT
0	16.45	16.46	16.88	15.77	16.31	17.30	16.47	16.53	17.01	16.38
1	10.48	10.45	10.20	8.32	10.39	9.52	7.83	10.18	9.25	7.73
2	0.78	0.85	0.85	1.76	0.85	0.59	1.52	0.77	0.77	1.71
3	0.35	0.25	0.11	0.47	0.31	0.17	0.50	0.29	0.11	0.41
4	0.26	0.23	0.22	0.10	0.27	0.25	0.17	0.24	0.22	0.14
5	0.23	0.16	0.14	0.18	0.23	0.10	0.16	0.23	0.11	0.17
6	0.17	0.20	0.12	0.09	0.19	0.16	0.12	0.21	0.11	0.11
7	0.12	0.12	0.16	0.06	0.11	0.19	0.11	0.08	0.14	0.13
8	0.12	0.15	0.11	0.06	0.19	0.20	0.08	0.16	0.12	0.04
9	0.13	0.18	0.15	0.18	0.18	0.14	0.12	0.15	0.14	0.09
10	0.18	0.17	0.08	0.05	0.16	0.08	0.02	0.16	0.06	0.05

(b) Phase(days)

Order	JMA	Buoy 1			Buoy 2			Buoy 3		
	AT	AT	SWT	BWT	AT	SWT	BWT	AT	SWT	BWT
0	-	-	-	-	-	-	-	-	-	-
1	33.30	34.84	42.75	50.08	35.31	44.66	51.04	36.48	47.10	52.40
2	-10.92	-6.36	10.27	20.32	-7.07	10.73	21.65	-3.12	18.73	23.46
3	-13.89	-13.47	1.11	-28.35	-8.20	-4.84	30.18	-13.13	-0.77	-28.80
4	-3.31	0.42	11.12	-13.25	1.12	6.59	-21.76	-0.88	7.54	20.85
5	1.08	-6.39	-4.92	7.22	-3.21	-7.89	3.20	-0.76	1.70	2.02
6	-1.75	-0.74	-1.92	-14.55	-3.92	-5.31	3.32	-1.95	0.36	9.52
7	-0.36	4.19	10.11	3.62	6.36	11.62	5.23	5.50	12.57	10.47
8	-10.93	-9.75	-8.26	-2.23	-9.53	-7.12	-8.74	-9.41	-3.67	-6.43
9	-2.43	-3.47	2.53	5.41	-2.58	2.04	4.82	-2.48	3.76	0.60
10	4.89	3.44	8.36	8.93	3.34	4.95	-5.17	3.31	7.65	-0.73

Reference: Order 0 = the mean value.. Based on the order 1 value (=annual cycle components), the values until the orders 2, 2, and 3 are higher than 5% of the order 1 air, surface and bottom water temperature's value. The values of the higher orders are remains below maximum 3% of the order 1 value of the air, surface and bottom water temperature's data.

Every air and water temperature data can be fitted by the harmonic analysis. It means the harmonic coefficients of order M are estimated based on the least square methods by using the following equations. The fitting function is composed by the linear combination of the harmonic constants and its frequency functions.

Equation (1) can be expressed as the following matrix form:

$$[T] = [A]\,[H] + [E] \quad (3)$$

in which, $[T] = [T_1, T_2, \ldots, T_N]^{tp}$ and is the temperature data (N×1) vector (known, observed), the superscript tp refers to the transpose of the matrix, and [A] = [I:C:S] expressed as follows:

$I = [1\ 1\ \ldots\ 1]^{tp}$, (N× 1 vector),

$$C = \begin{bmatrix} \cos(\omega_1 \cdot 1) & \ldots & \cos(\omega_M \cdot 1) \\ \cos(\omega_1 \cdot 2) & \ldots & \cos(\omega_M \cdot 2) \\ \vdots & \ddots & \vdots \\ \cos(\omega_1 \cdot N) & \ldots & \cos(\omega_M \cdot N) \end{bmatrix},$$

$$S = \begin{bmatrix} \sin(\omega_1 \cdot 1) & \ldots & \sin(\omega_M \cdot 1) \\ \sin(\omega_1 \cdot 2) & \ldots & \sin(\omega_M \cdot 2) \\ \vdots & \ddots & \vdots \\ \sin(\omega_1 \cdot N) & \ldots & \sin(\omega_M \cdot N) \end{bmatrix}, \quad (4)$$

in which, the matrix [A] is the [N×(2M+1)] matrix (known), $H=[A_0, A_1, A_2, \ldots, A_M, B_1, B_2, \ldots, B_M]^{tp}$ and is the harmonic coefficient [(2M+1)×1] matrix (unknown), and $[E] =[\epsilon_1, \epsilon_2, \ldots, \epsilon_N]^{tp}$ and is the residual (N×1) vector (unknown).

The coefficient matrix [H] can be estimated by following procedures (Hermance, 2007).

The objective function is

$$\text{Min}\{[E][E]^{tp}\}=\text{Min}\{([T]-[A][H])([T]-[A][H])^{tp}\}, \quad (5)$$

Where, Min{ } means the minimization of the { }, i.e., the optimization problem.

The optimal solution is obtained when the differentiation of the objective function, Eq. (5), with respect to [H] set to zero. It becomes [T] - [A][H] = [0]. It also can be written as [T] = [A][H]. It requires some matrix manipulation because the [A] is not square. Then, the solution for [H] becomes the equation (6) via the following step, $[A]^{tp}\,[T] = [A]^{tp}[A][H]$:

$$[H]=\{[A]^{tp}\,[A]\}^{-1}[A]^{tp}\,[T] \quad (6)$$

The results of the harmonic analysis including the optimal order, the AIC value, the residual variance, and the harmonic constants (amplitudes in ^{o}C and phases converted to the day units) are summarized in the Table 2. The optimal orders of the air and water temperatures are about 32-35 and 10-13, respectively. The value of the optimal order of the air temperatures is higher than that of the water temperatures. As shown in Figure 7, it is compared with the time-series plot between the observed data and the generated data with the optimal fitting curve, i.e., the linear combination of the harmonic functions of order 12. The intra-annual components, which mean the components having a longer than annual cycle, are not included because the available data seems not enough to analyze the long-term variation pattern although it makes the fitting-level (accuracy) better. The fitting-curve has an exactly same shape at 1-year interval in the condition that the harmonic analysis is carried out by using two or more year's data. It is the averaged fitting-curve during the total data periods.

The variances of the residuals are rapidly decreased until about order 3 to 5 and after constantly (a little bit slow) decreased as the harmonic order increases. In the perspective of the minimum residual variance, the higher the order is the better. Thus, the optimal model on this temperature data is decided based on the lowest AIC value widely used of the model selection criteria (Kitagawa, 2005). Basically, the harmonic analysis is the data-smoothing procedure like as the moving average and the data fitting based on the function. It is also very important process to analyze the data because the raw data having a high fluctuation are not suitable for the analysis of the overall variation pattern, such as the peak time, gradient, and time-delay, etc. The harmonic analysis model only gives the approximate variation by the combination of the harmonic functions.

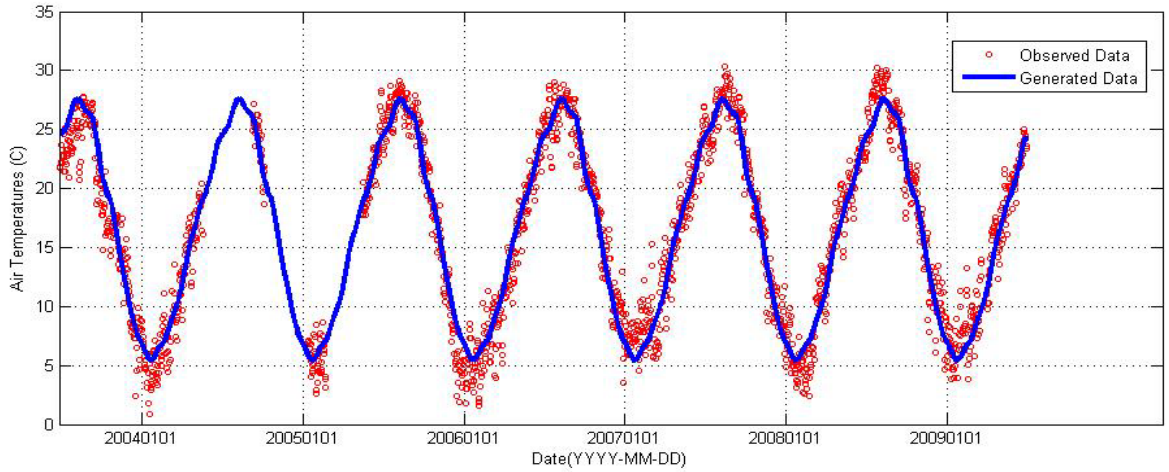

(a) Air temperature data in Buoy 1

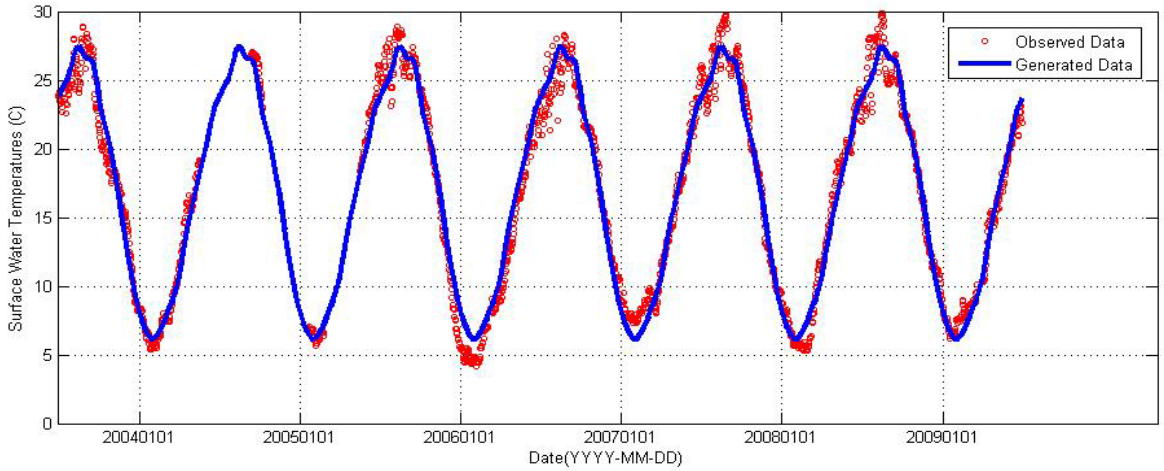

(b) Surface water temperature data in Buoy 1

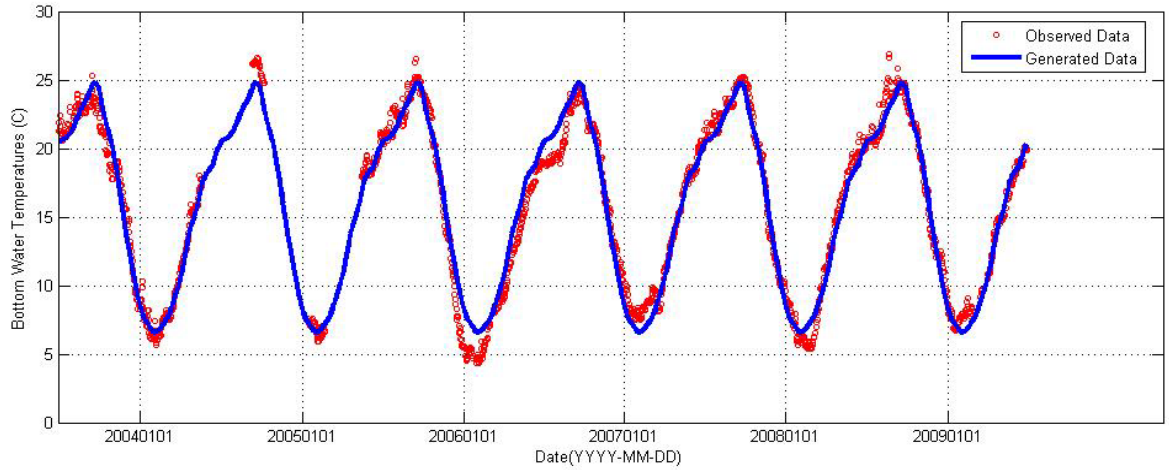

(c) Bottom water temperature data in Buoy 1

Figure 7. Comparison of the observed data and generated data by using the harmonic function

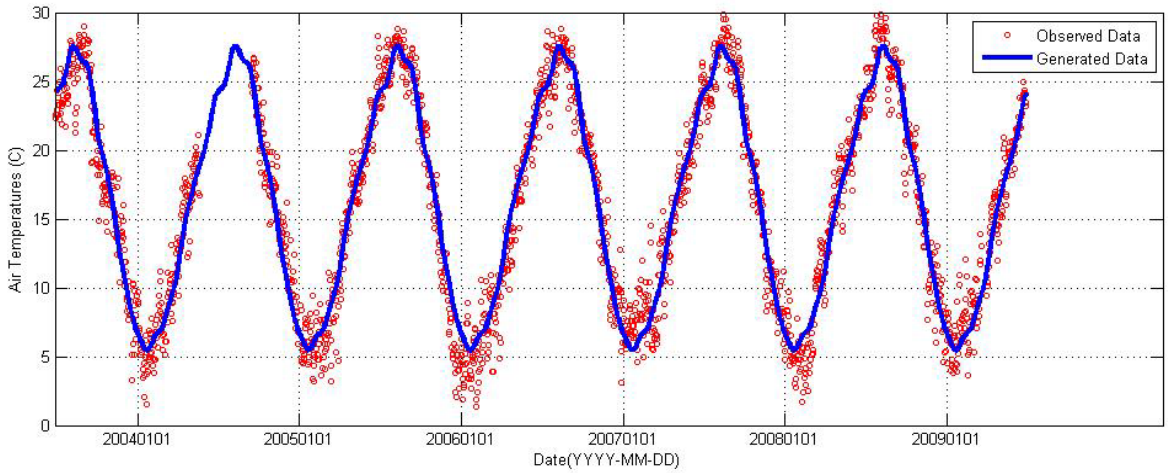

(d) Air temperature data in Buoy 2

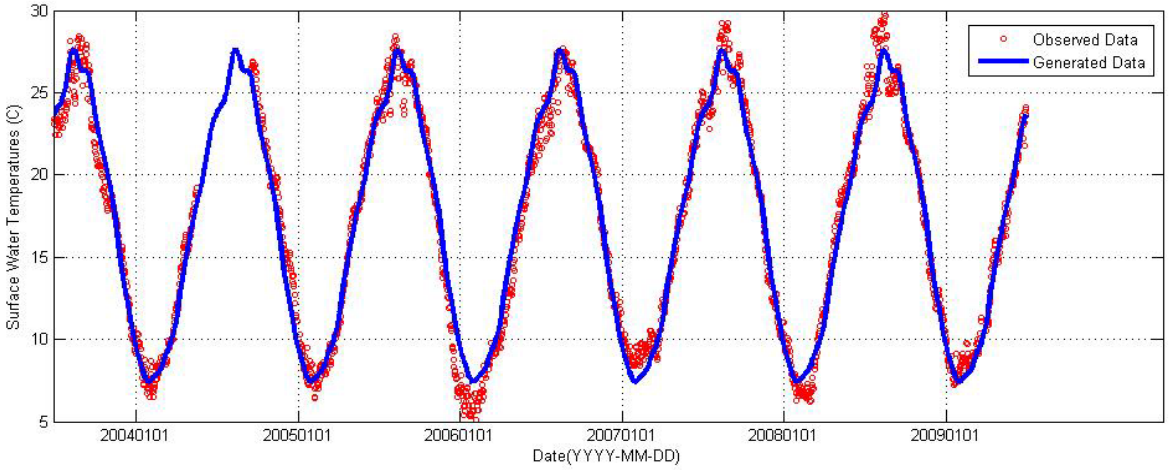

(e) Surface water temperature data in Buoy 2

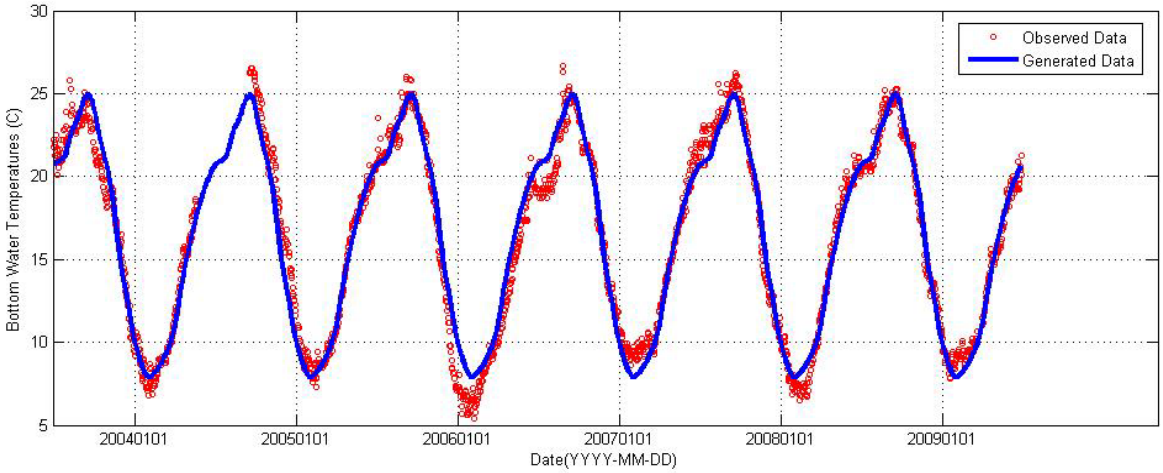

(f) Bottom water temperature data in Buoy 2

Figure 7. Comparison of the observed data and generated data by using the harmonic function (Continued)

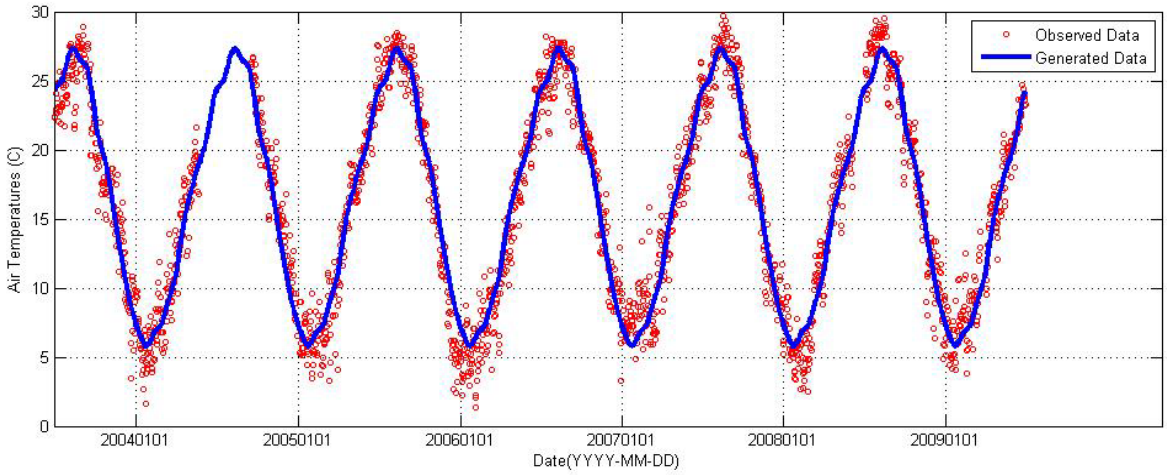

(g) Air temperature data in Buoy 3

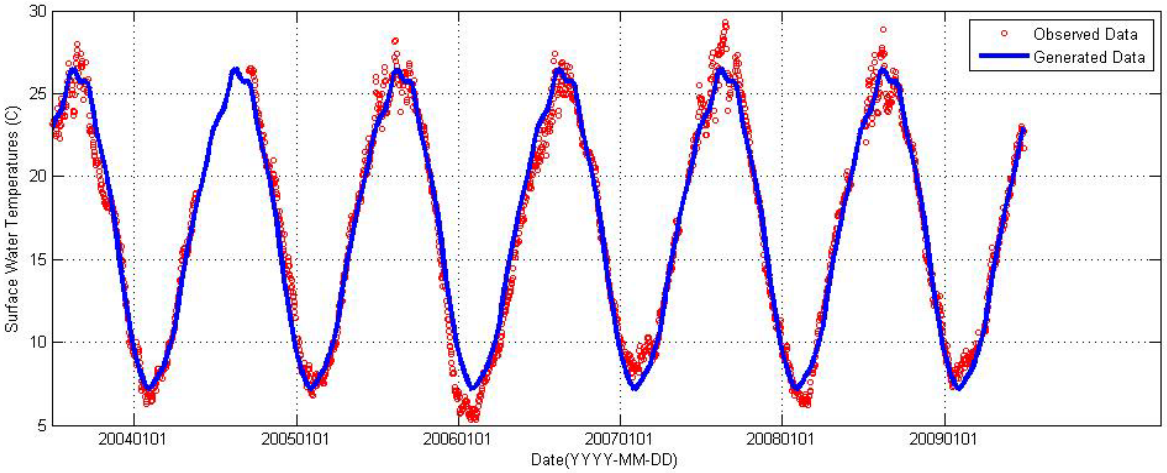

(h) Surface water temperature data in Buoy 3

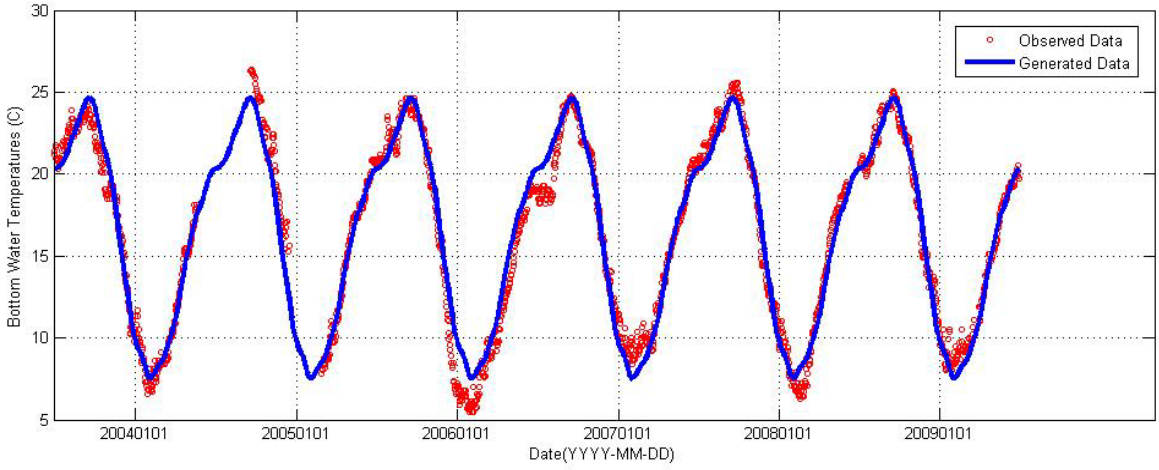

(i) Bottom water temperature data in Buoy 3

Figure 7. Comparison of the observed data and generated data by using the harmonic function. (Continued).

It does not give the relationship between air and water temperatures because the harmonic analysis is done independently by only using air and water temperatures data-set, respectively. Thus, it is required to establish the function-type relationship between air and water temperatures because of the estimation of the coastal water temperatures by only using the air temperatures. The data-fitting procedure is totally different from the estimation.

5. Loop model construction procedure

5.1 Loop construction by using the parametric form

The studies on the water temperature estimation using the air temperature data are mainly on the regression analysis, except to the numerical models. In general, the regression analysis method is widely used to find out the correlation degree between the parameters. However, it is not suitable for the time-series data because it cannot consider the temporal-variation pattern which is very important for the time-series data analysis.

Based on the results of the study using the regression curve, the single-valued curve is certainly not sufficient to express the relationship between air and water temperatures whether it is linear and non-linear curves or not. The hysteresis shape is the loop-type which cannot be expressed by the single-valued curve (Lapshin, 1995; Cruz-Hernandez and Hayward, 2001). In order to overcome these limitations, a loop-type function or any other multi-valued function should be checked. In this study, the loop function is suggested as these forms able to describe the loop, or ellipse forms, etc. In relation to this, the HL (hysteresis loop) model of order (m, n), HL(m,n), based on the loop function is suggested to describe the relationship between the air and water temperatures in the coastal zone. Even though the different orders between air and water temperatures can be used only to draw the more accurate hysteresis loop, the same order condition, i.e., m=n, is used in order to apply to the water temperature estimation explained in detail at the following section. HL(0,0) is the center point of the ellipse-type loop and HL(1,1) gives the ellipse shape. The optimal orders based on the lowest AIC value are about 36 for air temperature and 12 for water temperatures. In this study, every detailed analysis is carried out by using the HL(36,12) model. However, the same order is used to setup the HL model in this study even though the optimal order is different on air and water temperatures.

Previous studies:

$T_W(t) = aT_A(t)+b$ (linear equation),

$T_W(t) = a/(1+\exp[b(c-T_A(t))]$ (non-linear logistic equation).

In this study (Parametric form):

$$[T_W(t),T_A(t)]=[f_A(t), f_W(t)]=[HA(t), HW(t)] \quad (8),$$

in which, a, b, and c are the model parameters, and $f_A(t)$, $f_W(t)$ are the approximation or best-fitting (smoothing) function of the air and water temperature data, respectively. Basically, every possible function can be used only if it is considered as the approximate function of the time-series data. For example, the polynomial function fitting method, the moving-average smoothing methods, the time-series model, and the harmonic analysis, etc. In this study, the harmonic analysis is selected because it has an advantage of the component analysis of the time-series data. The functions, HA(t) and HW(t), are given as the following equation (9):

$$HA(t)-\mu_A= \sum_{m=1}^{M}\{CA_m \cos(\omega_m t) + SA_m \sin(\omega_m t)\}$$
$$HW(t)-\mu_W= \sum_{m=1}^{M}\{CW_m \cos(\omega_m t) + SW_m \sin(\omega_m t)\} \quad (9)$$

The above function HA(t), HW(t) can be determined by the harmonic analysis of the air and water temperature data. If the parametric form is used, the loop having a lot of shapes is constructed as the order of the harmonic function changes. The higher the order, the more complex the loop shape is. The simplest shape is the ellipse-type loop in order 1(see Fig. 8). The order 0 is the center point of the loop, i.e., the location of the mean air and water temperature values.

The only requirement of the HL model application is that the variation patterns and the changes of the air temperatures should be included in this function. In terms of the component comparison, the harmonic function is very useful and powerful even though the other approximate functions more closely fit the time-series air and water temperature data.

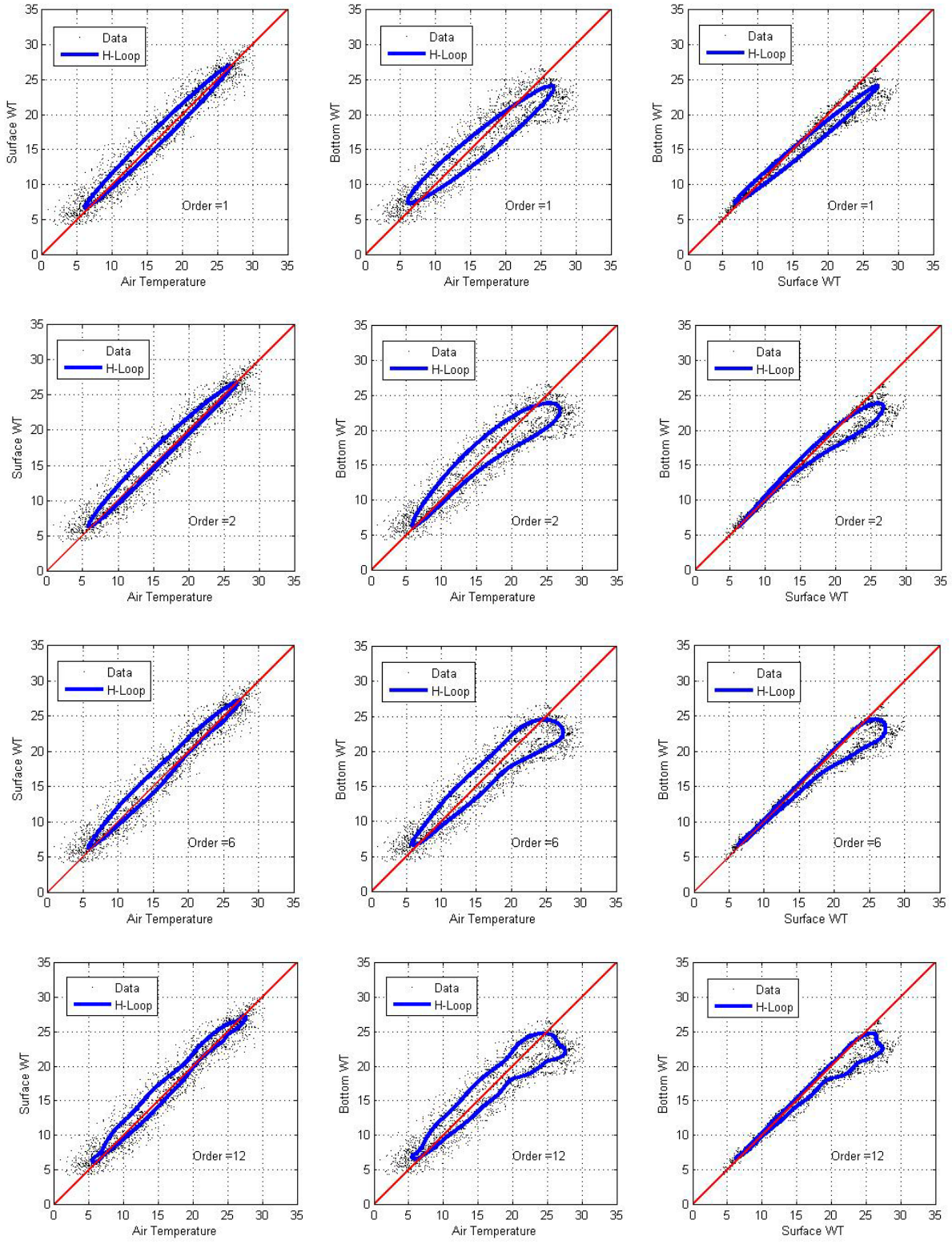

(a) Buoy 1

Figure 8. The shapes of the hysteresis-loop of orders 1, 2, 6, and 12.

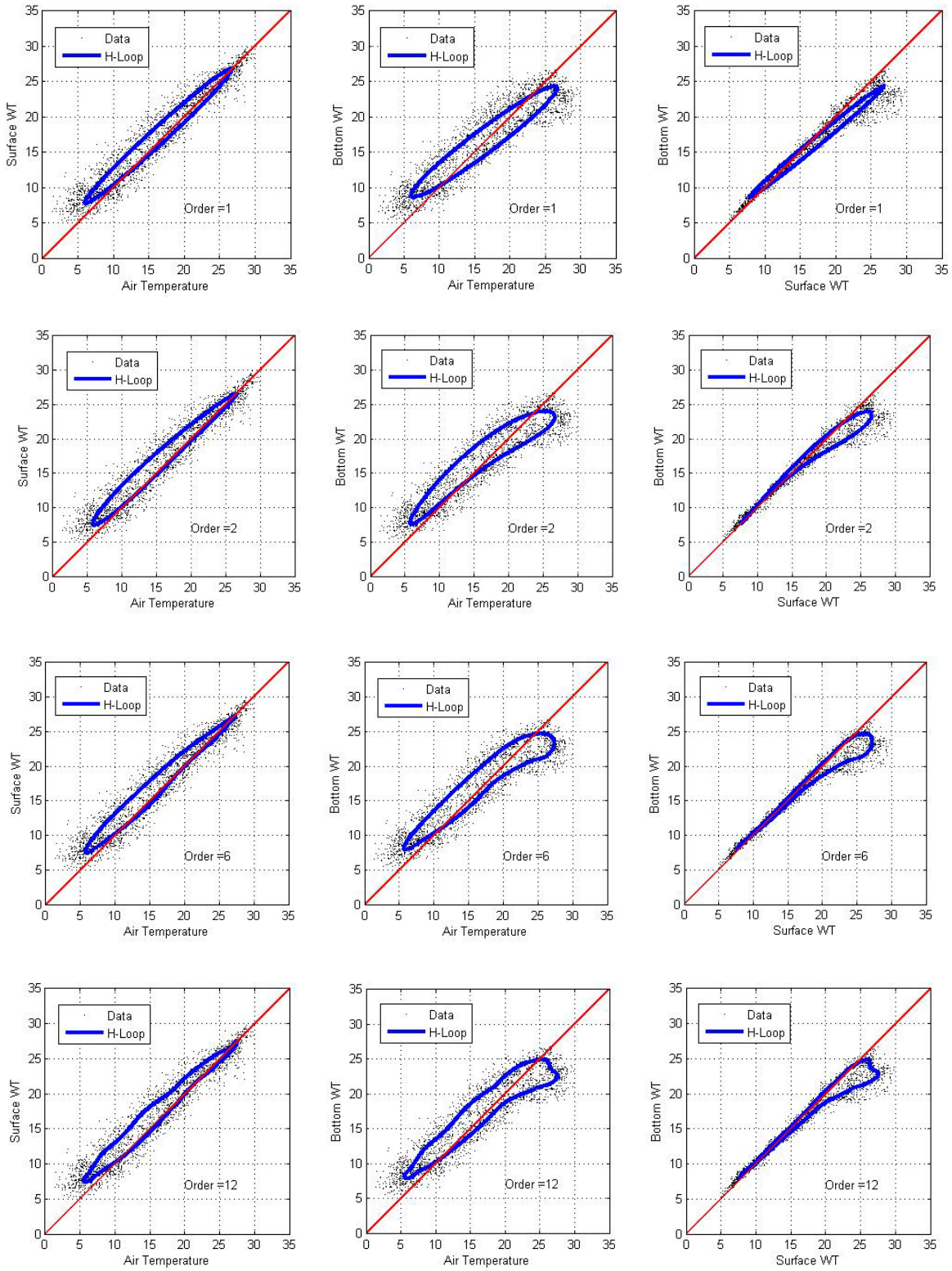

(b) Buoy 2

Figure 8. The shapes of the hysteresis-loop of order 1, 2, 6, and 12.

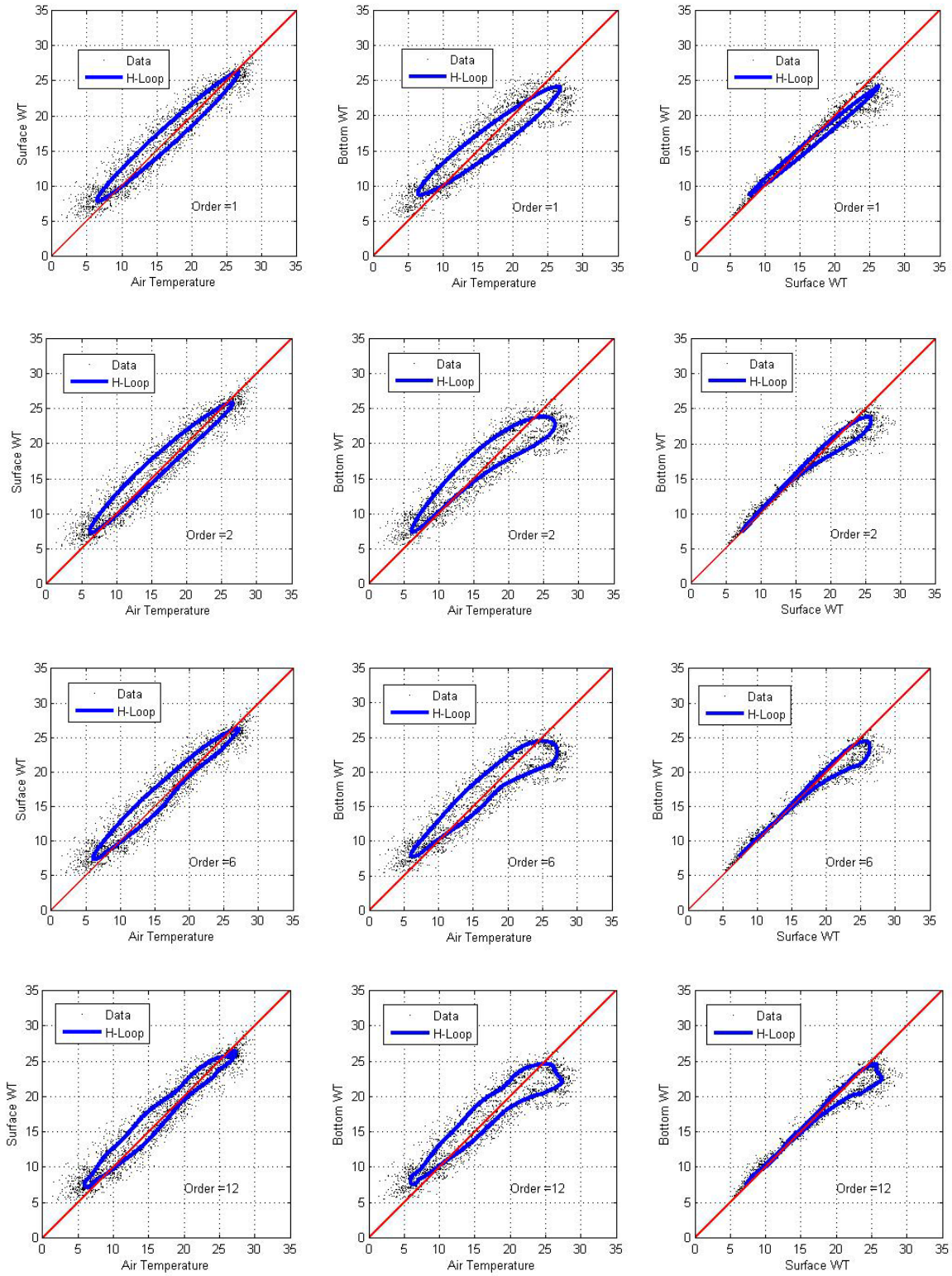

(c) Buoy 3

Figure 8. The shapes of the hysteresis-loop of order 1, 2, 6, and 12.

In the step of the model building, the HL model is easily established by the harmonic analysis of the each data set in the condition that the air and water temperature data are both available. However, in the application step, i.e., the estimation step, it becomes not available condition of the water temperature data. So, the loop function cannot be evaluated if the harmonic constants of the water temperature data are not provided. In relation to this problem, the practical (technical) estimation method of the harmonic constant of the water temperatures should be suggested.

This method is based on the constant ratio assumption of the harmonic constants between air and water temperatures. In this analysis, the ratio of the harmonic constants keeps approximately constant on the dominant (until 3-order) constants). The ratio becomes highly variable on the high order constants. However, the impact can be negligible because it is included in the residual fluctuation level. The ratio could be changed for the locations. However, the temporal ratio changes will be maintained nearly constant. It makes the HL model possible to estimate the water temperature using the air temperature data in the condition of the future changes and pattern changes. It should be checked in detail for more accurate and general applications. As another option, the difference HL method could be suggested based on the constant difference of the harmonic constants between air and water temperatures. It also is checked in the model application section.

5.2 Time-Lag analysis

It is very difficult to extract the time-lag information between the air and water temperatures raw data set because of the high fluctuation. When we use the harmonic functions, it is much easier to find out the time-lag because the fluctuation terms are smoothed by using the low-order harmonic coefficients. In this study, the fitting curves obtained from the harmonic analysis with the order 6 are used because the curves of higher-order coefficients make it more difficult. The time-lag analysis is carried out by using the harmonic functions of the air and water temperatures. The lag times (days) are obtained respectively in the rising and falling periods of the air temperature because it is different as the air temperature increases and decreases. The time-lag is analyzed only the air-surface water and surface-bottom water temperatures only. The time-lag is not constant. So, its mean value of the time-lag at 10, 15, 20 degrees in Celsius is used as the representative value. The time lag (delay) is defined as an amount of time in days that passes to reach the specified temperatures between air and water temperatures. In this study, the specified temperatures are the lowest and highest values, in order to analyze the seasonal time-lag variation patterns. Figure 9 shows the various time-lag definitions schematically. In general, the time lag defined in the highest and/or lowest point is widely used.

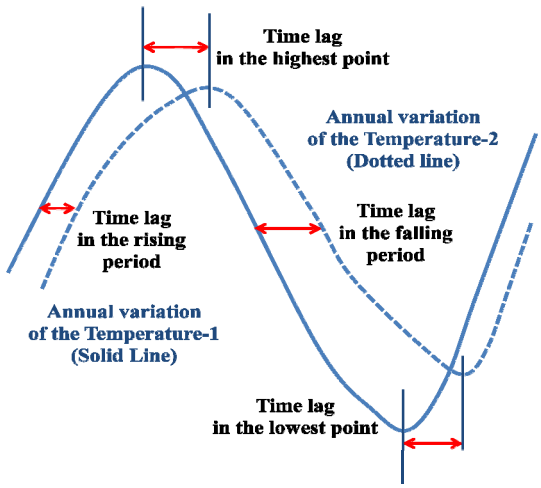

Figure 9. Schematic definition diagram of the time-lags between air and water temperatures

The time-lag, which unit is “day”, obtained based on the various time-lag definitions are summarized in the Table 4.

Table 4. Time-lags between the air and water temperatures.

		RP	HP	FP	LP
Buoy 1	AT-SWT	4.8	6.0	10.0	5.0
	SWT-BWT	12.5	35.0	1.9	1.0
Buoy 2	AT-SWT	1.5	3.0	8.8	3.0
	SWT-BWT	15.7	36.0	3.5	4.0
Buoy 3	AT-SWT	4.7	6.0	13.7	5.0
	SWT-BWT	7.2	32.0	1.7	-1.0

Reference: RP, HP, FP, and LP mean the time-lags (Unit: days) of the rising period, the highest time, the falling period, and the lowest time of the air and water temperatures, respectively.

The time-lag difference between AT-SWT is much bigger in the falling period than the rising period. It is reversely changed in the condition of the SWT and

BWT relationship. Especially, the time-lag between the maximum temperature's occurring dates becomes more than 30 days between SWT-BWT. It means the rising of the bottom water temperature is very slowly progressed by the heat transfer interception due to the thermal stratification in the summer season.

6. Model calibration and validation - model application

In the regression model, the water temperature from the air temperature can be directly estimated by the curve equation. However, the HL model estimates the water temperature as a time-series data. In the regression model, the air temperature change is directly influenced on the water temperature estimation. It is also required to make a relationship between the air and water temperatures in the HL model because the air temperature changes should be considered to the estimation of the water temperatures. In this study, the relationship is established by the ratios or differences of the harmonic coefficients of the air and water temperatures data even though it can be applied only in the condition of the nearly constant ratio. If the relationship is setup, the application (estimation) process of the HL model can be carried out by following steps:

Step 0: [Given condition] Air temperature data.
Step 1: Harmonic analysis of the air temperature time-series data. Harmonic constants are obtained.
Step 2: Harmonic constants of the water temperature are computed by the constant ratio or difference values which are already computed by using the existing data set. (in the model calibration stage.)
Step 3: HL loop is made by the harmonic constants of the air and water temperatures.

It is required to check the ratio (or difference) of the harmonic constants obtained from the air and water temperatures data in more detail. The information can be used to update the HL model application method by suggesting more reliable techniques. HL model is very easy to setup and more reasonable to show the synchronized changes (tracks) of the air and water temperature changes because the hysteresis pattern is considered whether its impact is large or not.

Basically, the ratio and difference of the harmonic constants is computed by using the 1-year harmonic analysis data in order to consider the typical annual temperature change patterns.

The ratio and difference between the harmonic constants of the air and water temperature data remain nearly constant until the order 2. The ratios become highly variable as the order increases above 3. However, the values of 0-th (mean value), 1st and 2nd order are dominant, even though the high fluctuation inhibits the HL model application. The absolute value of the harmonic coefficients of high order is below 0.5 and the harmonic constants of the 1st and 2nd order is the range 5 to 10 which is about 10-20 times greater than the high order harmonic coefficients.

The relationship setup process between air and water temperatures starts with the following equation:

$HW(t)\text{-}\mu_W = \sum_{m=1}^{M}\{CW_m \cos(\omega_m t) + SW_m \sin(\omega_m t)\}$.

It also becomes the following suggested forms,

$HW(t)\text{-}r_0\mu_A =$

$$\sum_{m=1}^{M}\{r_m CA_m \cos(\omega_m t) + r_m SA_m \sin(\omega_m t)\} \quad (10),$$

or

$HW(t)\text{-}d_0\mu_A =$

$$\sum_{m=1}^{M}\{d_m CA_m \cos(\omega_m t) + d_m SA_m \sin(\omega_m t)\} \quad (11)$$

in which, $r_m=W_m/A_m$, $d_m=W_m-A_m$, and the subscript m refers to the order of the harmonic functions, and the CW, SW, CA, and SA refer to the order m harmonic constants of the water and air temperatures data estimated in the harmonic analysis.

In this equation, r and d refer to the ratio and difference between the harmonic constants of the air and water temperatures, respectively. Thus, the HL model is classified as two types based on the harmonic constant computation methods. One is the HLM-R which means the HL model using the ratio method expressed as the equation (10), and the other is the HLM-D which means the HL model using the difference method expressed as the equation (11).

In order to estimate of the future water temperature changes, the harmonic constants of the water temperature data should be changed by the ratio and difference

which is already estimated by using the available air and water temperature data set. The harmonic constants of the future air temperature data are easily estimated by the harmonic analysis based on the least square methods, i.e., the equation (6).

This scatter plot is the comparison plot between observed and HL-model estimated values. In this scatter plot, the root-mean squared error (hereafter RMS error or RMSE) is computed by the root of the distance-square concept, as follows.

The RMSE is given by:

$$\mathrm{RMSE} = \sqrt{(\mathrm{WT_O} - \mathrm{WT_E})^2}$$

where, WT is the water temperature and the subscripts O and E refer to the observed and estimated values, respectively. Table 5 is the linear regression analysis information between air and water temperatures. The regression curves are used to estimate the surface and bottom water temperatures by using air temperatures. The comparisons of the observed and estimated temperatures are carried out in the calibration stage and validation (or verification) stages. The RMSE values of the liner regression method and HL model are summarized in the Table 6. (See also the Figure 10 and 11.) The RMS errors of the linear-regression method and HL model are on the range of 1.42–2.06, and 0.79–0.97, respectively. The HL model's results show better estimation results in comparison with the LRM. It is about 5% of the approximate temperature variation range, with respect to 30 degrees in Celsius.

The HL model is calibrated by using the data during 2005.7-2007.6 (2 year's data) and validated (verified) by using the data during 2007.7-2009.6 (also 2 year's data). The higher the order is, the lower the residual is and the oscillation of the estimation result is. Because of these characteristics, the HL model of order 10 is used to estimate the water temperatures even though the optimal order is about 12. The estimation pattern using HL model of higher order makes high frequency oscillations. This oscillation pattern should be checked and analyzed in detail whether it is significant or not, but it is skipped in this study.

Table 5. Regression analysis information between the air and water temperatures.

Buoy No.	Data Items	Equations of the regression curve	R^2
Buoy 1	AT – SWT	$(SWT)_{B1} = 0.9285\cdot(AT)_{B1} + 1.3845$	0.9380
	AT - BWT	$(BWT)_{B1} = 0.7336\cdot(AT)_{B1} + 3.4766$	0.8434
Buoy 2	AT – SWT	$(SWT)_{B2} = 0.8796\cdot(AT)_{B2} + 2.9322$	0.9320
	AT – BWT	$(BWT)_{B2} = 0.7015\cdot(AT)_{B2} + 4.9055$	0.8455
Buoy 3	AT – SWT	$(SWT)_{B3} = 0.8470\cdot(AT)_{B3} + 2.8388$	0.9140
	AT - BWT	$(BWT)_{B3} = 0.6893\cdot(AT)_{B3} + 4.8366$	0.8326

Reference: AT, SWT, and BWT are the air temperature, surface and bottom water temperatures, respectively. The subscripts, B1, B2, and B3 mean the Buoy 1, Buoy 2, and Buoy 3, respectively. R^2 is the coefficient of the determination.

Table 6. Root-mean-squared errors of the estimation by the linear regression method and the HL model.

Buoy No.	Items	Calibration stage		Validation stage		
		LRM	HLM	LRM	HLM-D	HLM-R
Buoy 1	AT – SWT	1.500	0.972	1.415	0.937	0.864
	AT – BWT	2.062	0.972	1.838	0.856	1.418
Buoy 2	AT – SWT	1.482	0.820	1.360	0.852	0.921
	AT – BWT	1.946	0.874	1.765	0.835	1.240
Buoy 3	AT – SWT	1.532	0.847	1.557	0.860	0.762
	AT - BWT	1.903	0.872	1.794	0.788	1.102

References: AT, SWT, and BWT are the air temperature, surface and bottom water temperatures, respectively. LRM and HLM are the linear regression method and the hysteresis loop model, respectively. D and R refer to the difference and ratio method, respectively, i.e., the water temperature's harmonic constant computation method in the HL model.

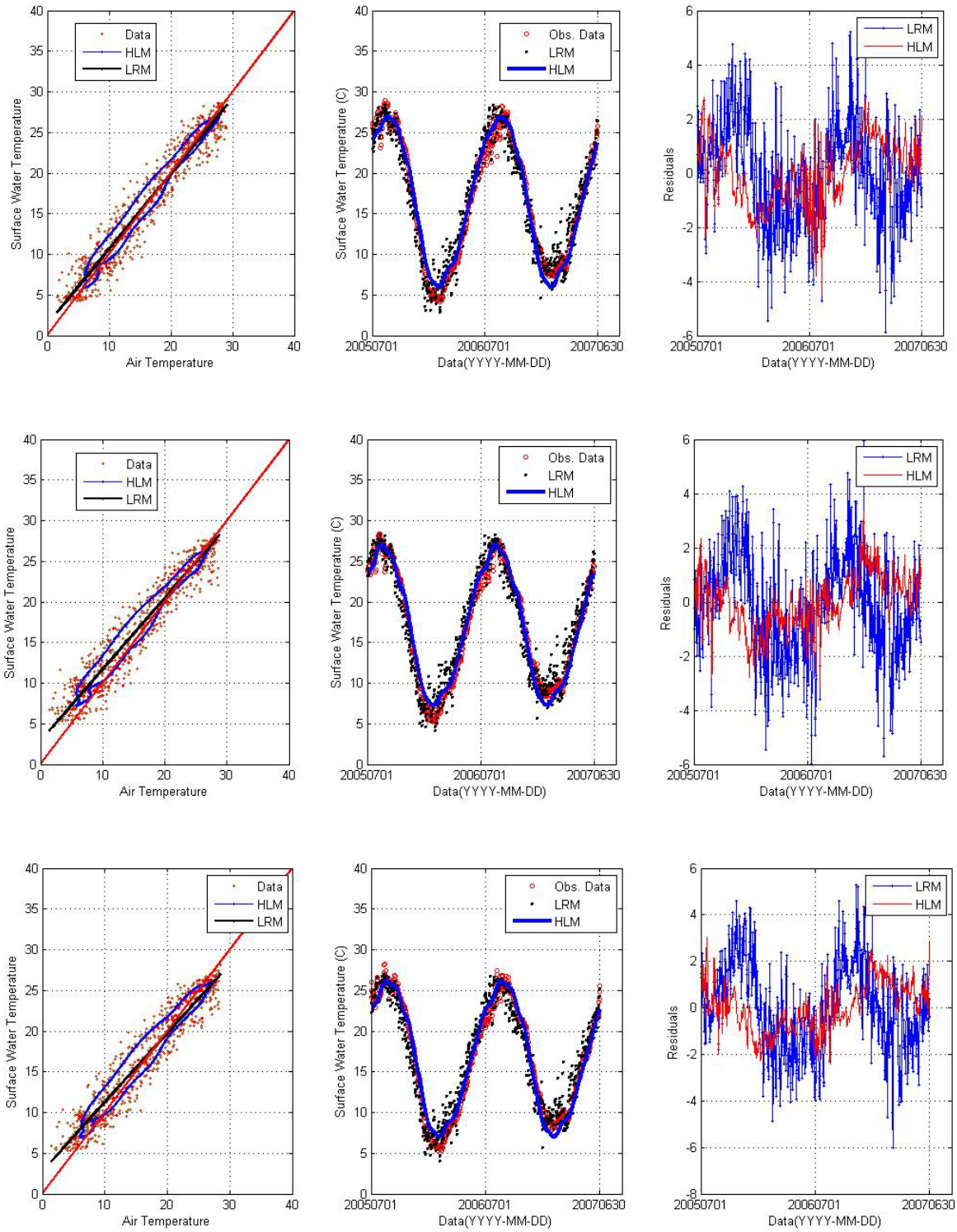

(a) Surface water temperatures

Figure 10. Comparison plot between observed and estimated data for the model calibration.

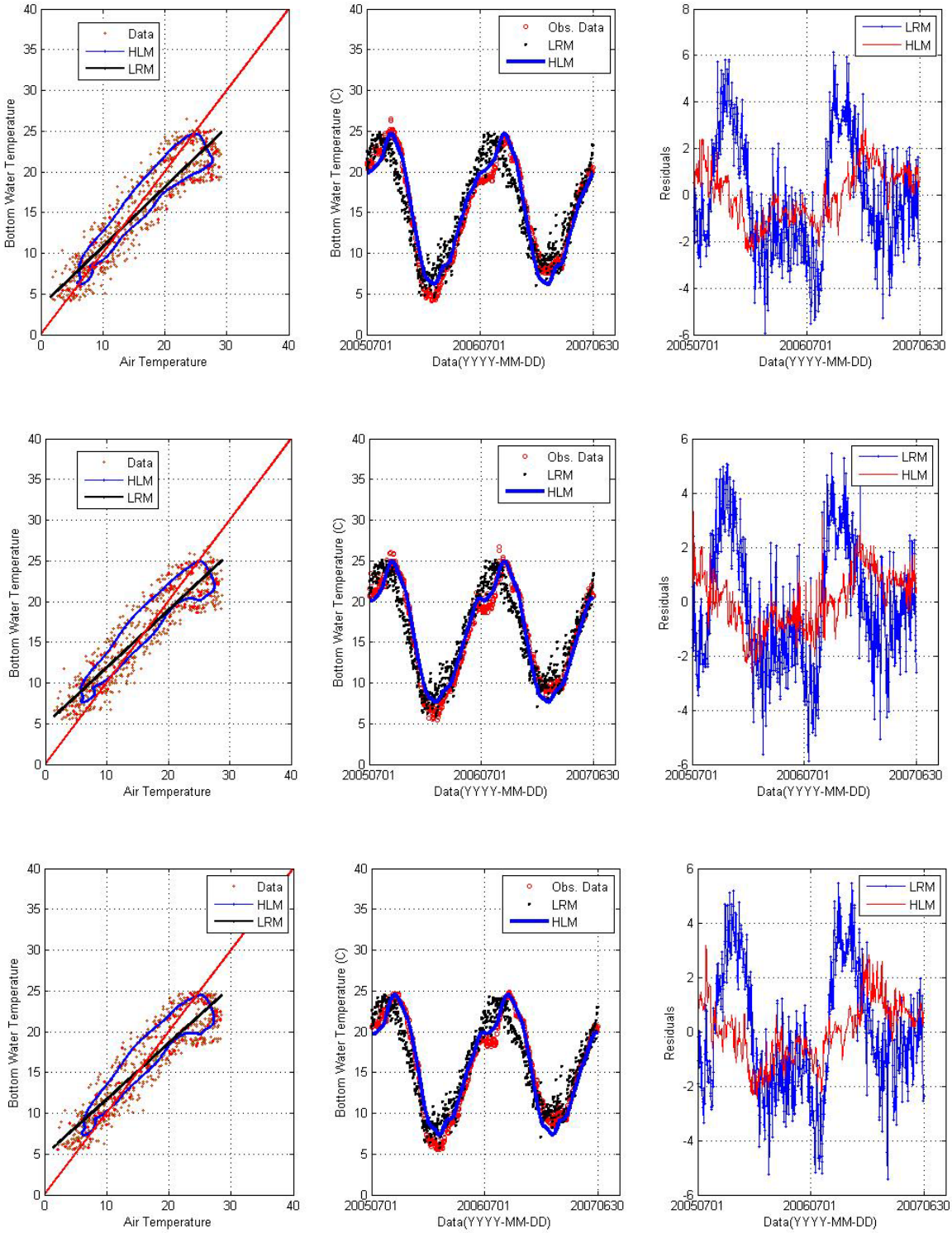

(b) Bottom water temperatures

Figure 10. Comparison plot between observed and estimated data for the model calibration (Continued).

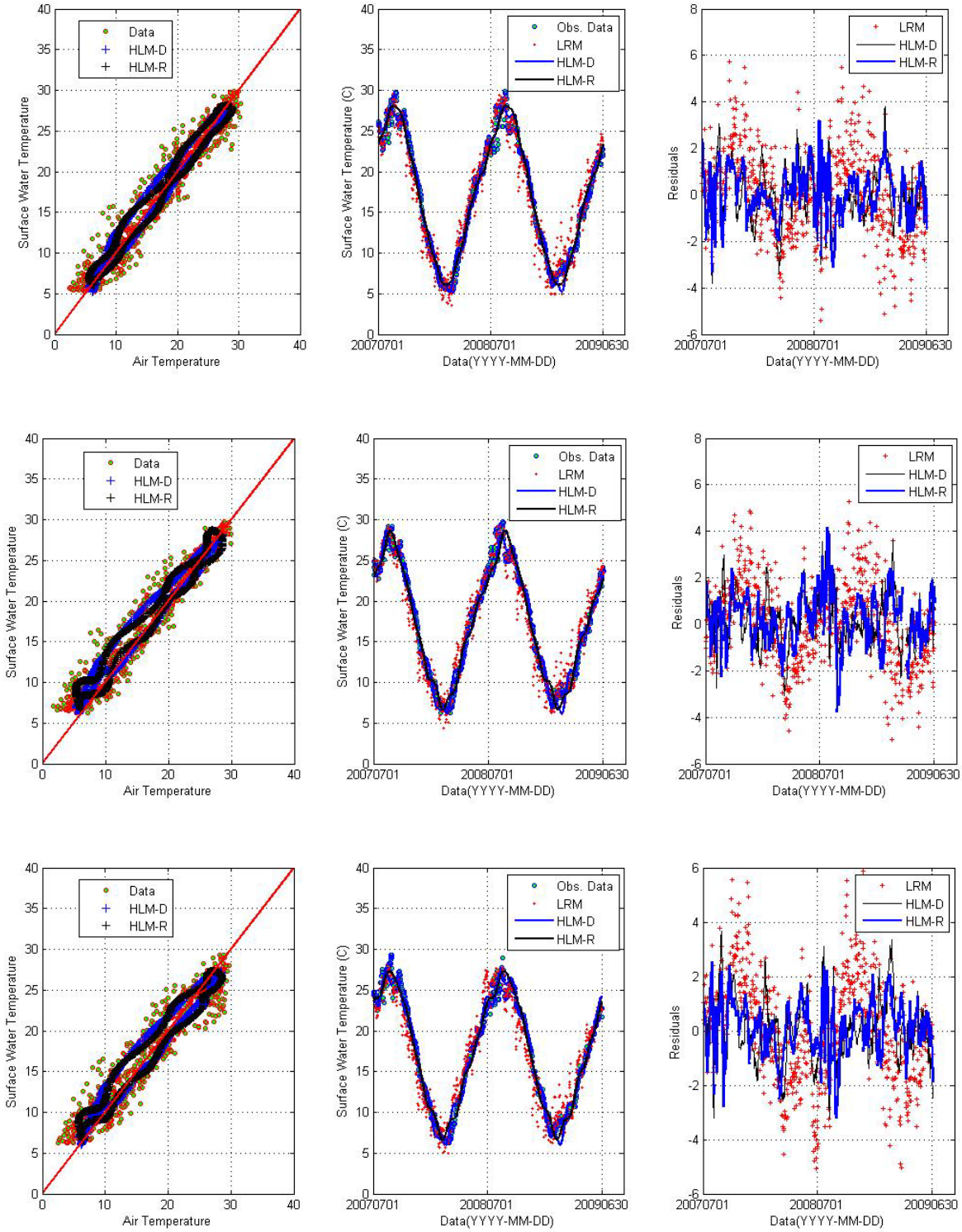

(a) Surface water temperatures

Figure 11. Comparison plot between observed and estimated data for the model validation.

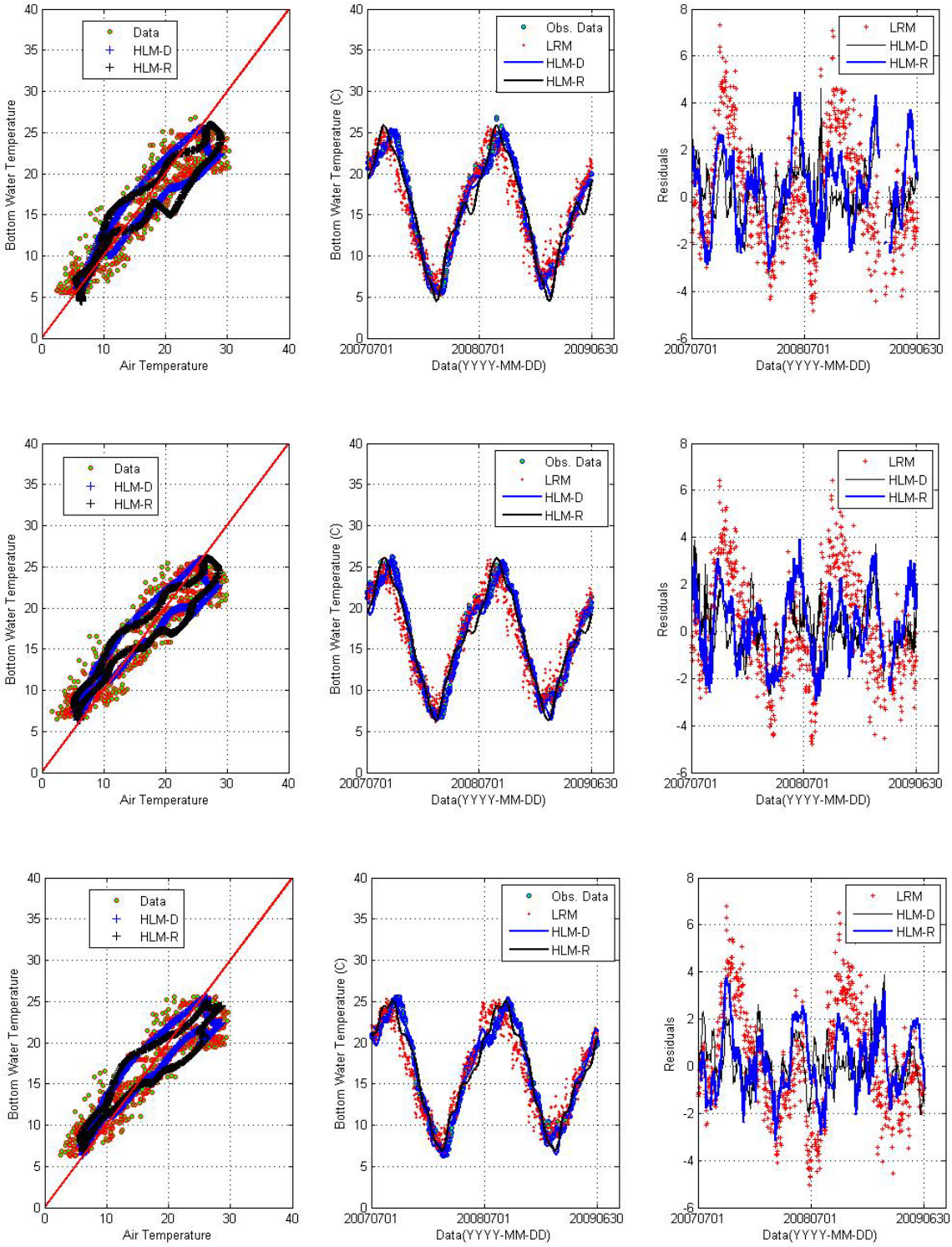

(b) Bottom water temperatures

Figure 11. Comparison plot between observed and estimated data for the model validation (Continued).

Figures 10-11 show the comparison between observed and estimated data of the water temperature. As shown in this figures, the estimated data by using the linear-regression method also included in order to compare the typical estimation method. As expected, the systematic bias between the observed and estimated data using the regression method is clearly appeared. On the contrary, the estimated data with HL model show that the variation pattern are more close to the observed data in terms of the typical time-lag and hysteresis and the RMSE is lower than that of the LRM.

Since the HL type model is not suggested before, the more detailed analysis is required. It remains as the future research topics, such as the relationship between the air and water temperature variation structure, the other method for computation of the harmonic constants, the residual analysis based on the phenomena and data fluctuation, the method for the addition of the another factors, and the limitation of the HL model in terms of the basic concept and model application.

7. Conclusions

The hysteresis loop model able to estimate the coastal water temperature only with the air temperature data is suggested. It is also calibrated and validated to test the model reliability level by using the buoy monitoring data in Mikawa Bay, Japan. This model is able to consider the hysteresis which cannot be considered in the regression-type model in terms of the concept. The model calibration and validation results show that the HL model has higher estimation level than that of regression model.

For a model validation, the coastal water temperatures are estimated in this period, 2007.7-2009.6, only from the same period time-series data of the air temperature by the HL model developed in this study. The estimation results are well fitted of the monitored water temperature data at a range of the 0.8-1.0 RMS errors. The method based on the constant difference option is proved to give better estimation results than that of the method based on the constant ratio option.

The model could be improved and modified based on the more diverse, spatially and temporally, coastal water temperature data analysis, because the site-specific factors are very important in the coastal zone. However, a kind of the universal relationships also may be obtained by the more in-depth study because the heat transfer mechanism in the coastal zone is the physical phenomena expressed as the heat-energy conservation equation.

Addition of the other factors which are expected to have substantial effects on the variation of the coastal water temperature, such as (warm or cold) ocean current, mixing intensity by the wind or flow in a certain depth, and any other artificial causes, makes the model prediction ability certainly improved. However, every modification should be suggested and applied based on the practical point of view, i.e., data availability. As the kind of data or parameters required in the model run increases, the uncertainty level also increases because of the poor data condition.

In conclusion, it is expected to be increased the application level and field of the HL model via the appropriate combination of the other methods predicting the water temperatures, e.g., numerical models. That is the why every model and method has an advantage and disadvantage.

Acknowledgements

The authors are also thankful to Dr. Masahiko Furuichi, Director for special research of PARI, Dr. Kitazume Masaki .

(Received on . , 2009)

References

Barnett, V. and Lewis, T. (1994). Outliers in Statistical Data, Third Edition, John Wiley & Sons.

Berner, E.K. and Berner, R.A. (1987): The Global Water Cycle, Geochemistry and Environment, Prentice-Hall, Inc.

Benyahya, L., Caissie, D., St-Hilaire, A., Ouarda, T.B.M.J., and Bobee, B., (2007). A Review of Statistical Water Temperature Models, Canadian Water Resources Journal, 32(3), pp.179-192.

Cho, H.Y., Lee, K.H., Cho, K.J., and Kim J.S. (2007): Correlation and Hysteresis Analysis between Air and Water temperatures in the Coastal Zone - Masan Bay, J. of Korean Coastal and Ocean Engineering, KSCOE, 19(3), pp.213-221 (in Korean).

Crisp, D.T. and Howson, G. (1982): Effect of air temperature upon mean water temperature in streams in the north Penninines and English Lake District, Freshwater Biology, 12, pp.359-367, Blackwell.

Cruz-Hernandez, J.M. and Hayward, V. (2001.1): Phase control approach to hysteresis reduction, IEEE Transactions on Control Systems Technology, 9(1), pp.17-26.

Department of Ecology, State of Washington, (2009): A citizen's guide to understanding and monitoring lakes and streams, http://www.ecy.wa.gov/programs/wq/plants/management/joysmanual/streamtemp.html

Hermance, J.F. (2007): Stabilizing high-order, non-classical harmonic analysis of NDVI data for average annual models by damping model roughness, International Journal of remote Sensing, 28(12), pp.2801-2819.

Hsu, S.A. (1988): Coastal Meteorology, Academic Press.

Kitagawa, G. (2005): A Premier of the Time-series Analysis, Sec. 5.3. (in Japanese).

Knauss, J.A. (1978): Introduction to Physical Oceanography, Chapter 3, Prentice-Hall Inc.

Kyle, R.E. and Brabets, T.P. (2001): Water temperature of streams in the Cook Inlet basin, Alaska, and Implications of Climate Change, Water - Resources Investigation Report 01-4109, U.S. Department of the Interior, U.S. Geological Survey.

Lalli, C.M. and Parsons, T.M. (1997): Biological Oceanography, An Introduction, Chapter 2, 2nd Edition, Butterworth-Heinemann

Lapshin, R.V. (1995): Analytical model for the approximation of hysteresis loop and its application to the scanning tunneling microscope, The Review of Scientific Instruments (Rev. Sci. Instrum.). 66(9), pp.4718-4730, American Institute of Physics.

Lee, K.H. (2007. 4.): Nonlinear correlation analysis between air and water temperatures in the coastal zone, Korea, J. of Korean Coastal and Ocean Engineering, KSCOE, 19(2), pp.128-135 (in Korean).

Little, R.J.A. and Rubin, D.B. (2002): Statistical Analysis with Missing Data, Part I, 2nd Edition, John-Wiley & Sons, Inc.

Mohseni, O., Stefan, H.G., and Erikson, T.R. (1998). A nonlinear regression model for weekly stream temperatures, Water Resources Research, 34(10), pp.2685-2692.

Morrill, J.C., Bales, R.C. and Conklin, M.H. (2005). Estimating stream temperature from air temperature: Implications for future water quality, J. of Environmental Engineering, 131(1), pp.139-146.

Murphy, S. (2009): General Information on Temperature. http://bcn.boulder.co.us/basin/data/COBWQ/info/Temp.html

Pilgrim, J.M. and Stefan, H.G. (1995): Correlation of Minnesota stream water temperatures with air temperatures, Project Report 382, St. Anthony Falls Lab., Univ. of Minnesota, Minneapolis.

Poff, N.L., Brinson, M.M., and Day Jr., J.W. (2002): Aquatic ecosystems & Global climate change; Potential Impacts on Inland Freshwater and Coastal Wetland Ecosystem in the United States, Pew Center on Global Climate Change.

Stefan, H.G. and Preud'home, E.B. (1993): Stream temperature estimation from air temperature, Water Resources Research, 29(1), pp.27-45.

United Nations Environment Programme (2007): Global Environment Outlook – environment for development (GEO-4), Chapter 4. Water, UNEP Report.

Weber, K., Sturmer, L., Hoover, E., and Baker, S. (2007): The Role of Water Temperature in Hard Calm Aquaculture, FA 151, University of Florida, IFAS Extension.

港湾空港技術研究所報告　第 49 巻第 2 号

２０１０．６

編集兼発行人　独立行政法人港湾空港技術研究所

発　行　所　独立行政法人港湾空港技術研究所
横須賀市長瀬３丁目１番１号
TEL. 046(844)5040 URL. http://www.pari.go.jp/

印　刷　所　株式会社　大　應

CONTENTS